Published in final edited form as:
Dev Biol. 2009 February 1; 326(1): 86–100. doi:10.1016/j.ydbio.2008.10.033.

Notch regulation of progenitor cell behavior in quiescent and regenerating auditory epithelium of mature birds

Nicolas Daudet[1,2], **Robin Gibson**[3], **Jialin Shang**, **Amy Bernard**[3], **Julian Lewis**[1], and **Jennifer Stone**[3]

1 *Vertebrate Development Laboratory, Cancer Research UK, London*

2 *Centre for Auditory Research, UCL Ear Institute, University College London, London*

3 *Virginia Merrill Bloedel Hearing Research Center and Department of Oto-HNS, University of Washington, Seattle, WA*

Abstract

Unlike mammals, birds regenerate auditory hair cells (HCs) after injury. During regeneration, mature non-sensory supporting cells (SCs) leave quiescence and convert into HCs, through non-mitotic or mitotic mechanisms. During embryogenesis, Notch ligands from nascent HCs exert lateral inhibition, restricting HC production. Here, we examined whether Notch signalling (1) is needed in mature birds to maintain the HC/SC pattern in the undamaged auditory epithelium or (2) governs SC behavior once HCs are injured. We show that Notch pathway genes are transcribed in the mature undamaged epithelium, and after HC injury, their transcription is upregulated in the region of highest mitotic activity. In vitro treatment with DAPT, an inhibitor of Notch activity, had no effect on SCs in the undamaged epithelium. Following HC damage, DAPT had no direct effect on SC division. However, after damage, DAPT caused excessive regeneration of HCs at the expense of SCs, through both mitotic and non-mitotic mechanisms. Conversely, overexpression of activated Notch in SCs after damage caused them to maintain their phenotype and inhibited HC regeneration. Therefore, signalling through Notch is not required for SC quiescence in the healthy epithelium or to initiate HC regeneration after damage. Rather, Notch prevents SCs from regenerating excessive HCs after damage.

Keywords

Notch; lateral inhibition; hair cell; regeneration; chicken; transdifferentiation; progenitor

INTRODUCTION

In mammals, production of mechanosensory hair cells (HCs) in the cochlea is completed before birth. Any subsequent loss of auditory HCs is not corrected, resulting in permanent hearing loss. In contrast, many non-mammalian vertebrates readily regenerate HCs into adulthood

Corresponding Author: Jennifer S. Stone, Ph.D., Research Associate Professor, CHDD CD176 Box 357923, Virginia Merrill Bloedel Hearing Research Center, Department of Otolaryngology/Head and Neck Surgery, University of Washington, Seattle, WA 98195-7923, Phone: 206-616-4108 FAX: 206-221-5685, e-mail: stoner@u.washington.edu.

(reviewed in Stone and Cotanche, 2007). A central problem in hearing research is to understand the mechanisms that dictate whether or not lost HCs are replaced.

Hair cell regeneration has been most thoroughly studied in birds. In the avian auditory epithelium (basilar papilla, or BP), progenitors of new HCs are supporting cells (SCs), which reside amongst HCs. All SCs of the BP are formed and differentiated by hatching (Katayama and Corwin, 1989; Ginzberg and Gilula, 1979; Goodyear et al., 1996). After hatching, SCs normally remain quiescent (Oesterle and Rubel, 1993), but if HCs are destroyed, SCs give rise to new HCs in two distinct ways. Initially, some SCs convert into HCs without dividing, a processed termed *direct transdifferentiation* (Adler and Raphael, 1996; Roberson et al., 1996). A couple of days later, additional SCs divide, and their progeny differentiate into HCs or SCs (Corwin and Cotanche, 1988; Hashino and Salvi, 1993; Raphael, 1992; Ryals and Rubel, 1988; Stone and Cotanche, 1994). In this manner, a balanced mixture of HCs and SCs cells is reestablished, and thereafter, the system returns to quiescence.

Little is known about the signals that regulate the behavior of mature SCs, in quiescence or after HC loss. Clues may be derived from embryogenesis. In all vertebrates, sensory patches of the inner ear originate as groups of progenitor cells that then diversify to form a precisely patterned mosaic of HCs and SCs. A critical regulator of this process is the Notch pathway. Notch signalling depends on transmembrane ligands of the Delta or Serrate/Jagged family, expressed on signal-delivering cells, which bind to Notch receptors in signal-receiving cells (reviewed in Lewis, 1996). This triggers a series of gamma-secretase-dependent cleavages that release the intracellular fragment of Notch, called N^{ICD}. N^{ICD} translocates to the nucleus and stimulates expression of transcriptional effectors of the *Hes/her/E(spl)* family, which in turn regulate the expression of downstream target genes. Through this mechanism, a cell expressing a Notch ligand and differentiating into a particular cell type can inhibit its neighbors from doing likewise, a phenomenon called lateral inhibition (Artavanis-Tsakonas et al., 1995; Kageyama et al., 2005; Lewis, 1998).

Many studies have shown that lateral inhibition regulates the embryonic production of HCs (reviewed in Kelley 2006). Newly formed HCs express the proneural gene *Atoh1*, which is required for HC specification and/or differentiation (Bermingham et al., 1999; Millimaki et al., 2007), and they also express two Notch ligands, Delta1 (Dll1) and Serrate2/Jagged2 (Adam et al., 1998; Lanford et al., 1999; Lanford et al., 2000; Morrison et al., 1999; Zine and de Ribaupierre, 2002). These ligands activate Notch in neighboring cells, stimulating *Hes1* and *Hes5* expression. Hes1 and/or Hes5 repress the HC fate (Zheng et al., 2000; Zine et al., 2001), inhibiting expression of *Atoh1* and *Dll1*. As a result, cells contacting HCs remain as progenitors or, later, differentiate as SCs (Woods et al., 2004; Yamamoto et al., 2006; Takebayashi et al., 2007; Hayashi et al., 2008). On the other hand, disruption of Notch signalling in the embryonic inner ear results in excessive production of HCs. Lateral inhibition via Notch also appears to regulate progenitor cell division in developing epithelia of the inner ear (Kiernan et al., 2005; Takebayashi et al., 2007) and during regeneration in lateral line neuromasts (Ma et al., 2008).

Although Notch-pathway genes are expressed in inner ear epithelia post-embryonically (Stone and Rubel, 1999), the specific roles for Notch in maintenance and repair of the HC-SC pattern in inner ear epithelia capable of HC regeneration have not been studied. Here, we examined the expression of several Notch pathway components in the mature chicken BP, in the normal state and during regeneration after HC loss, and we tested the consequences of blocking Notch signalling in each condition. We found that Notch activity is not required to maintain mature SCs in quiescence, to reactivate progenitor cells (SCs) after HC injury, or to directly regulate progenitor cell (SC) division after HC injury. Instead, Notch activity modulates the number of

SCs that directly transdifferentiate into HCs, as well as the number of SC progeny that differentiate into HCs, after damage has occurred, in a region-specific manner.

MATERIALS AND METHODS

Animal care and treatment

Fertile eggs of chickens (*Gallus gallus*, White Leghorn) were received from Hyline International (Graham, WA). Post-hatch chicks between days 5 and 10 received Gentamicin (subcutaneous, 1 × 250 mg/Kg on 2 consecutive days, Sigma-Aldrich, St. Louis, MI) and/or bromodeoxyuridine (BrdU; intraperitoneal, 100 mg/Kg, Sigma-Aldrich, St. Louis, MI) as per Stone and Rubel (2000). Chickens were euthanized by intraperitoneal Nembutal overdose or decapitation, conforming to AALAC standards. Tissue was dissected and fixed in buffered 4% paraformaldehyde (Stone and Rubel, 1999; Stone et al., 2000).

Tissue Labeling

Proteins were detected in whole-mount cochlear ducts using indirect immunolabeling. Rabbit anti-Atoh1 antibody was received from Dr. Jane Johnson (University of Texas Southwestern Medical Center). Mouse anti-HCA, anti-SCA, and anti-β-Tectorin-Precursor-like antibodies were received from Dr. Guy Richardson (University of Sussex, UK). Rabbit anti-MyosinVI antibody was purchased from University of California San Diego (Dr. Tama Hasson) or Proteus Biosciences (Ramona, CA). Mouse anti-GFP antibody was purchased from Molecular Probes (Eugene, OR). Mouse or rat anti-BrdU antibodies were purchased from BD Sciences (San Jose, CA), DAKO (Glostrup, Denmark), or SeraLabs (West Sussex, UK). Rabbit anti-Caspase 3 antibodies were purchased from R & D Systems (Minneapolis, MN). Secondary antibodies conjugated to fluorophores (Cy3, Cy5, Alexa 488) were purchased from Jackson ImmunoResearch Laboratories (West Grove, PA) or Molecular Probes (Eugene, OR). Atoh1 immunolabeling was performed as described in Cafaro et al. (2007). The TUNEL reaction, with fluorescent detection (Chemicon, Temecula, CA), was used to detect dying cells in whole-mount cochlear ducts.

mRNA was detected in whole-mount cochlear ducts using non-radioactive in situ hybridization (ISH; Stone and Rubel, 1999; Henrique et al., 1995). Digoxygenin (DIG) or Fluorescein (FITC)-conjugated riboprobes were synthesized from plasmids containing fragments or complete cDNA of the following chicken genes: *Serrate1*, *Delta1*, *Notch1*, *Hes5.1* and *Hes5.3* (obtained from Dr. Domingos Henrique; University of Lisbon, Lisbon, Portugal), *Lunatic Fringe* (*Lnfg*; obtained from Dr. Cliff Tabin, Harvard University), and *Atoh1* (obtained from Fernando Giraldez from Pompeu Fabra University, Barcelona, Spain). Riboprobes were detected using Alkaline Phosphatase-conjugated anti-DIG antibody and NBT/BCIP substrate (Roche, Indianapolis, IN), or anti-DIG and anti-FITC antibodies conjugated to Horseradish peroxidase (HRP; Roche, Indianapolis, IN), and Tyramides labeled with Cy3 or FITC (TSA Plus fluorescence system; Perkin Elmer, Waltham, MA). Sense probes served as negative controls. For double-ISH, specimens were hybridized with a mixture of DIG- and FITC-labeled RNA probes that were detected sequentially. After revealing the first probe, specimens were incubated in Glycine/2N HCl and washed before applying the second horse radish peroxidase-conjugated antibody. Following ISH, some samples were processed for immunolabeling with rabbit anti-Serrate1 (Adam et al., 1998) and/or mouse anti-BrdU (DAKO; Glostrup, Denmark) antibodies.

To examine gene/protein expression after in vivo Gentamicin exposure, approximately 8 BPs were examined per time-point and gene. To compare gene/protein expression in DMSO-treated (control) and DAPT-treated BPs, at least 5 specimens from the same culture batch were processed in parallel (2–3 culture runs were performed per experiment).

Purification of mRNA and preparation of cDNA

For each condition (control, 1 day post-Gentamicin, or 4 days post-Gentamicin), sensory epithelium (BP) from the proximal half of the cochlear duct was isolated as described in Stone et al. (1996). For each run (n=3 per condition), tissue from 22 cochlear ducts was placed directly in RNeasy R1 Buffer (Qiagen, Valencia, CA) and stored at −80°C. RNA was isolated using the RNeasy Micro kit (Qiagen, Valencia, CA). RNA quality and yield were confirmed using a ND-1000 spectrophotometer (NanoDrop Technologies, Wilmington, DE). First-strand cDNA was synthesized using PowerScript Reverse Transcriptase (Clontech, Mountainview, CA), diluted 1:20 in 10 mM Tris-HCl, 0.1 mM EDTA (pH 8.0), and stored at −20°C.

Quantitative real-time polymerase chain reaction (qRTPCR)

For each qRTPCR run, approximately 60 ng of cDNA were used. Amplification was performed using an iCycler (BioRad, Hercules, CA). Primer sets (Invitrogen, Carlsbad, CA; Table 1) were designed to have comparable melt curves (Tm = 60°C). Samples lacking Reverse Transcriptase treatment or cDNA template served as negative controls. Threshold cycle (Ct) was set at 300 relative fluorescent units. *β-actin* was confirmed as a strong reference gene across control and Gentamicin-treated samples using geNorm software (http://medgen.ugent.be/~jvdesomp/genorm/).

To estimate changes in mRNA levels after Gentamicin treatment, the $2^{-\Delta\Delta Ct}$ method was used (Pfaffl, 2001; Colebrooke et al., 2007). For each sample, the mRNA level of each target gene relative to *β-actin* was estimated by calculating the DeltaCt, or ΔCt ($Ct_{Target\ Gene} - Ct_{\beta\text{-}actin}$) and then converting to $2^{-\Delta Ct}$. These values were averaged across samples in a group (n=3), and statistical differences were examined using ANOVA. To compare mRNA levels between experimental groups, the ratio of the average $2^{-\Delta Ct}$ for each treatment group relative to the control group ($2^{-\Delta\Delta Ct}$) was determined for each gene. This ratio represents a fold change for each gene after damage.

Organ culture, DAPT treatment, and electroporation

Cochlear ducts were isolated, the tegmentum vasculosum was removed, and organs were cultured free-floating in 500 μl of Dulbecco's Minimal Essential Medium (Sigma/Aldrich, St. Louis, MI) at 37°C in 95% air/5% CO_2. These drugs were added to media: 1% Fetal Bovine Serum (Atlanta Biologicals, Atlanta, GA), Penicillin/Streptomycin (1% or 78 μM Streptomycin, Sigma-Aldrich, St. Louis, MI), 5-bromo-2-deoxyuridine (BrdU, 1 μM, Sigma-Aldrich, St. Louis, MI), and N-[N-(3,5-Difluorophenacetyl-L-Aalanyl)]-S-phenylglycine t-butyl ester (DAPT, 1 μM–100 μM, Calbiochem #565770, San Diego, CA) dissolved in Dimethyl Sulfoxide (DMSO, 0.1%–1%, Sigma-Aldrich, St. Louis, MI). Half-volumes of culture media were exchanged daily. For each experiment, at least 3 runs were performed. For each run, at least 6 organs were included for each experimental condition. Negative controls for DAPT consisted of DMSO at concentrations matching experimentals (0.1–1.0%).

After two days of culture in Streptomycin, some cochlear ducts were electroporated with plasmid DNA. One of two plasmids driving expression of the intracellular domain of the chicken Notch1 receptor was used: *pN^{ICD}-IRES-EGFP* (Daudet and Lewis, 2005) *or pCAB-N^{ICD}-IRES-EGFP*. As a control vector, we used *pMES-IRES-EGFP* (from Dr. Catherine Krull, University of Michigan). All plasmids were delivered at similar concentrations (2–4 μg/μl). Organs were placed in a 10-μl drop of DNA (in TE buffer) on a plastic dish, and fine tungsten electrodes were placed on either side of the organ (approximately 1 mm apart), flanking the inferior and superior cartilaginous plates. Current was delivered using an ECM 830 BTX electroporator (Genetronics) with the following parameters: 60–75V, 60 ms duration, 100 ms inter-pulse duration, and 6–8 pulses per train. Current was delivered to three regions along the length of the BP (proximal, middle, and distal). In each region, three current trains were

delivered, then the polarity was reversed, and three additional trains were delivered. Following electroporation, organs were returned to the incubator for 2 or 5 additional days; media were replenished every two days.

Imaging and data analysis

Whole-mount cochlear ducts were imaged using laser scanning confocal, wide-field epifluorescence, and/or bright-field microscopy. For qualitative analyses, at least 6 organs were examined for each variable. For quantitative analyses, at least 3 organs were studied for each variable; numbers are provided below. Data were statistically analyzed by ANOVA (Fisher's PLSD) using Statview; s.d.'s are provided.

For quantitative analysis of *Hes5* and BrdU double-labeling, 7 cochlear ducts at 3 days post-Gentamicin/2 hours post-BrdU were analyzed. The entire damaged region was scanned at 60X. Each clearly identifiable BrdU-positive nucleus was scored as positive or negative for *Hes5*.

To determine the fate of transfected cells, each cochlear duct was analyzed at 40–60X on the confocal microscope. GFP-immunoreactive (IR) cells in the BP were identified, and healthy-looking cells (those lacking blebs, odd shapes, or other signs of damage) were chosen for further analysis. Each GFP-IR cell was scored as MyosinVI-negative or -positive and for whether its shape was more characteristic of a SC (bipolar cell with long apical and/or basal processes), HC (fusiform or round in shape), or atypical of either cell type. For the *pMES* group, we scored 138 GFP-IR cells (28 fields, 13 BPs), and for the p^{NICD} group, we scored 65 GFP-IR cells (23 fields, 15 BPs). For each field, we calculated the percentage of cells that were MyosinVI-negative or MyosinVI-negative.

To quantify BrdU/MyosinVI or BrdU/Atoh1 labeling, between 3 and 4 BPs from each group (DAPT, DMSO) were imaged using confocal microscopy at 60X. For each BP, two or three 41,209 μm^2 regions (proximal, mid-proximal, and/or middle) were analyzed. As a result, approximately 8–13% of the lesion's area was analyzed. All sites were situated halfway between the neural and abneural edges of the BP. Z-series stacks were obtained by scanning from the lumenal surface to the basal lamina. Counts were made off-line using ImageJ/Cell Counter. For each BP, an average count was obtained by pooling data from all sites. For BrdU counts, all BrdU-positive nuclei were included, regardless of their MyosinVI or Atoh1 labeling. For counting regenerated HCs, each MyosinVI-positive cell or Atoh1-positive cell was scored as BrdU-positive or -negative.

RESULTS

Several Notch pathway components are expressed in the quiescent basilar papilla at low levels and are upregulated after damage

In a previous study (Stone and Rubel 1999), we used ISH to examine expression of *Notch1*, *Delta1*, and *Serrate1* mRNA in mature chicken BPs that were either undamaged or damaged with the ototoxin, Gentamicin. Here, we expanded this analysis with a more sensitive method, qRTPCR, to quantify the changes in sensory epithelial expression of a larger set of Notch-related genes. We examined the following transcripts: *Notch1*, *Notch2*, *Delta1*, *Serrate1*, *Serrate2*, *Hes5*, *Hes6*, and *Atoh1*, as well as *Lnfg (*Haltiwanger, 2002) and *MINT (*Kuroda et al., 2003), which encode two modulators of Notch signalling. For reference, we also measured relative expression of *β-tectorin*, which is abundant in supporting cells (SCs)(Goodyear et al., 1996), and *MyosinVI*, which is expressed in hair cells (HCs)(Hasson et al., 1997).

We analyzed control (undamaged) BPs and regenerating BPs at 1 day and 4 days post-Gentamicin. To induce HC damage, we injected chicks with Gentamicin, once per day for 2 consecutive days, which causes complete HC loss throughout the proximal half of the BP but

preserves HCs in the distal half (Fig. 1A,B)(e.g., Cafaro et al., 2007). Since Gentamicin induces a reliable HC lesion only in the proximal half of the BP, all qRTPCR analyses were performed on RNA extracted from this region only.

The expression level for each Notch pathway transcript relative to *β-actin* ($2^{-\Delta Ct}$) is shown in Fig. 2A, as are expression levels for reference genes *β-tectorin* and *MyosinVI*. In the control BP, in which SCs are quiescent, *β-tectorin* was slightly more highly expressed than *β-actin*, and *MyosinVI* showed considerably lower expression. *Notch1*, *Notch2*, and *Serrate1* were the most strongly expressed Notch-pathway genes, and *Serrate2*, *Delta1*, *Atoh1*, *Hes5*, *Hes6*, *MINT*, and *Lnfg* were expressed at considerably lower levels.

By 1 day post-Gentamicin (measured from the first injection), direct transdifferentiation of SCs, but not SC division, is initiated in the damaged area (Cafaro et al., 2007; Roberson et al., 2004; Stone et al., 1999). At this time, expression of *Atoh1* mRNA was increased roughly 5-fold over levels in undamaged BPs, reflecting the initiation of HC production by direct transdifferentiation (Fig. 2A,B). A similar result was reported for Atoh1 protein at this time (Cafaro et al., 2007). In addition, expression of *Hes5* was significantly decreased compared to controls (to approximately 1/3X). However, none of the other genes in our analysis were significantly changed (by a factor of 2 or more, up or down) compared to controls at this time.

At 4 days post-Gentamicin, many SCs are dividing, additional SCs continue to undergo direct transdifferentiation, and specification of post-mitotic cells as either HCs or SCs is underway (Fig. 1C,D)(Stone and Rubel, 1999; Stone et al., 1999; Stone and Rubel, 2000). At this time, we saw statistically significant increases in the expression of several Notch-related genes relative to control BPs, including *Notch1* (1.7X) *Delta1* (3.5X), *Atoh1* (21.5X), *Hes5* (2X), *Hes6* (26X), and *Lfng* (4.7X) (Fig. 2A,B). Changes in *Notch2*, *Serrate1*, *Serrate2*, and MINT were seen, but they were not statistically significant ($p>0.05$).

The early upregulation of *Atoh1* at 1 day post-Gentamicin might be taken as a sign that a Notch-mediated lateral inhibition has been relieved following HC damage. However, our data show that this early change in *Atoh1* expression precedes changes in the expression of Notch ligands, suggesting that the effect is triggered not by disappearance of the ligands that activate Notch but by some other type of signal associated with HC damage. It is only later, as shown by our data at 4 days post-Gentamicin, that the Notch signalling pathway becomes strongly upregulated, when both direct transdifferentiation and mitotic regeneration of HCs are in full swing.

Expression of Notch pathway components in the damaged epithelium is spatially patterned

To localize Notch pathway gene expression in control BPs and after Gentamicin treatment, we performed whole-mount in situ hybridization and immunocytochemistry. Results are shown in Fig. 3, with panels A,F,K, and O illustrating the approximate region of the proximal BP where images were taken. For reference, we included images of MyosinVI (Fig. 3B,G) and BrdU **(**Fig. 3C,H) labeling to illustrate the degree of HC retention and SC division, respectively, seen in the proximal end of control and damaged samples. By 3–4 days post-Gentamicin, all HCs have been extruded from the proximal end of the BP, and SCs are actively dividing there, particularly in the neural half of the BP.

Our previous study using in situ hybridization showed that, in the control, undamaged BP, transcripts for *Notch1* and *Serrate1* are expressed in SCs, but *Delta1* mRNA is not detected in any cells (Stone and Rubel, 1999), which is consistent with our qRTPCR results. Further analysis here showed that Serrate1 protein is abundant in SCs throughout the control BP (Fig. 3D), but transcripts for *Lnfg* and *Hes5.3* are not detected (Fig. 3E,L). In contrast, *Hes5.1*-expressing cells were diffusely scattered throughout the BP (Fig. 3M). Staining in the lagena

provided a positive control for these results. In the lagena, a vestibular epithelium located in the distal end of the cochlear duct, there is continual HC turnover, and Serrate1 protein and *Hes5.3*, *Hes5.1*, and *Lnfg* mRNA were all strongly expressed there (data not shown). From these findings, we infer that in the quiescent auditory epithelium, some Notch pathway components are expressed and the pathway may have a low level of activity.

At 3 days post-Gentamicin, Stone and Rubel (1999) showed that expression of *Serrate1* and *Notch1* was not significant altered, but *Delta1* was highly upregulated throughout the area of HC loss, in a salt and pepper pattern. *Delta1* was transcribed in some S-phase cells at a low level, and it becomes highly upregulated in regenerated HCs as they differentiate. In this study, we examined whether labeling for Serrate1 protein or *Lnfg, Hes5.1, or Hes5.3* mRNA was altered at 1 or 2 days post-Gentamicin relative to controls. As judged by ISH, none of these Notch pathway components showed a significant change at these times, except for *Lnfg* mRNA, which was slightly upregulated in the damaged region of some BPs (data not shown). However, at 3–4 days post-Gentamicin, all of these Notch pathway components (Serrate1 protein and *Lnfg, Hes5.3*, and *Hes5.1* mRNA) showed significant upregulation in expression, particularly in the neural region of the BP (Fig. 3I,J,P,Q,R). This area has the highest level of mitotic activity after damage (Fig. 3H)(Cafaro et al., 2007). Double-labeling for *Delta1* and *Hes5* (using a cocktail of *Hes5.1* and *Hes5.3* probes) showed that *Hes5*-positive cells were typically *Delta1*-negative, and vice-versa (Fig. 3N), indicating that *Hes5*-positive cells were most likely SCs. No change in expression of any transcript or of Serrate1 protein was seen in the distal, undamaged region after Gentamicin treatment (data not shown). These findings demonstrate that, by the time SC division is initiated, Notch activity has become highly upregulated in SCs in the region of cell division. This upregulation may occur via Delta1 and/or Serrate1, which are also upregulated in this region.

Cell proliferation is stimulated in parallel with expression of Notch pathway components

After Gentamicin treatment, HC loss starts at the proximal end of the BP and spreads distally over time. At 4 days post-Gentamicin, SCs along the leading, distal edge of the lesion are undergoing the initial phase of HC regeneration (direct transdifferentiation), while SCs in more proximal regions are in later phases of regeneration, including SC division (Cafaro et al., 2007). To determine which SC behaviors are associated with increased Notch activity, we injected birds with BrdU at 4 days post-Gentamicin and killed them 2 hours later, to catch SCs in S-phase. We then double-labeled BPs for BrdU and *Hes5*, *Delta1*, or Serrate1.

In the middle of the damaged region (Fig. 4A–C), where Serrate1, *Hes5*, and *Delta1* were strongly expressed, we saw many BrdU-positive cells. This observation suggested that dividing SCs may have a high level of Notch activation. However, when we scored BrdU-labeled cells according to their level of Notch activation, as indicated by *Hes5* expression, we found that most cells showed labeling for only one of these two markers. Of 1574 BrdU-positive cells examined in 7 BPs, the majority of BrdU-positive cells were *Hes5*-negative (Fig. 4B inset); only 85 cells (5%) were *Hes5*-positive. Conversely, numerous BrdU-labeled cells expressed *Delta1* (Fig. 4C inset), confirming a similar observation by Stone and Rubel (1999) and indicating that their level of Notch activation was low. These data show that dividing cells tend to have low levels of Notch activity, as reflected by *Hes5* transcription. This suggests that 1) Notch activation is antagonistic toward SC re-entry into the cell cycle or 2) some damage-induced signal other than Notch activity provokes SC re-entry into the cell cycle and antagonizes *Hes5* expression.

Further analysis showed that Serrate1 and BrdU labeling shared a similar boundary (Fig. 4D), suggesting that Serrate1 upregulation occurs concurrent with SC re-entry into the cell cycle. In contrast, upregulation of *Hes5* (Fig. 4E) and *Delta1* (Fig. 4F) was seen in regions distal to Serrate1 upregulation, presumably along the leading edge of HC damage. This pattern of

expression mirrors that of Atoh1 protein after an identical HC damage paradigm (Cafaro et al., 2007).

Inhibition of gamma secretase in undamaged auditory epithelium does not trigger HC production

The expression of several Notch-pathway genes in the undamaged BP raised the question of whether Notch signalling plays any part in maintaining SCs in a quiescent state. To find out, we maintained cochlear ducts from post-hatch chickens in vitro in the presence of the gamma-secretase inhibitor, DAPT, which prevents the release of the activating intracellular fragment of Notch, the N^{ICD} (Dovey et al., 2001; Selkoe and Kopan, 2003). We compared the outcome of the DAPT treatment with that seen after similar culture in DMSO control medium.

In initial experiments, cultures were maintained for 3 or 7 days without Streptomycin or any other HC-damaging toxin, then fixed and immunolabeled for MyosinVI to detect HCs (Hasson et al., 1997). After 3 days of culture in DMSO control media, the morphology and patterning of the original HCs were retained in middle (Fig. 5A) and distal regions of the BP, but some HC damage and loss were evident in the proximal area (Fig. 5B). This damage was likely due to dissection or the lack of necessary trophic factors in culture media. The appearance of the BP after a similar time in medium containing 100 μM DAPT was comparable in both regions (Figs. 5C,D), indicating that DAPT, even at a high concentration, does not induce HC damage or trigger regenerative processes such as conversion of SCs into HCs.

In BPs cultured without Streptomycin for 7 days with DAPT (10 or 100 μM) or DMSO, original HCs in middle and distal parts of the BP were preserved (Fig. 5E, 10 μM DAPT is shown). In addition, these regions showed little evidence of new HC production after treatment with DMSO or DAPT, at either concentration (Fig. 5E,F). Newly differentiated HCs would have emerged in either the HC or SC nuclear layer as MyosinVI-positive cells that were smaller and more fusiform than original HCs (e.g., see Stone and Rubel, 2000). These findings demonstrate that inhibition of gamma secretase does not alter the normal state of the mature BP when original HCs are intact. Similar experiments accompanied by continuous BrdU labeling demonstrated that DAPT treatment in organs not exposed to Streptomycin does not trigger any discernible SC proliferation in undamaged areas (data not shown). Therefore, we conclude that, although several Notch pathway components are expressed in the mature undamaged BP, Notch signalling (at least, the canonical, gamma secretase-dependent type) is not responsible for maintaining SCs in a quiescent state.

The appearance of the proximal BP at 7 days in vitro, where culture conditions had caused nearly complete HC loss in both DMSO controls and DAPT-treated BPs, provided a marked contrast. Here, significant numbers of original HCs had died and been extruded (Fig. 5G,I). In BPs treated with DMSO (Fig. 5G,H), occasional regenerated HCs were seen in regions of HC loss. In contrast, in BPs treated with 10 or 100 μM DAPT, much higher numbers of regenerated HCs were seen in the proximal region, with the effect increasing with higher DAPT doses (Fig. 5I,J, 10 μM DAPT is shown). Therefore, although DAPT treatment is not sufficient to promote SCs to leave quiescence when local HCs remain intact, DAPT treatment does cause SCs to form excessive new HCs when local HCs are damaged or missing. This finding is examined in more detail below.

Inhibition of gamma secretase leads to increased *Atoh1* and *Delta1* expression and decreased *Hes5* expression after drug-induced HC loss

Next, we tested whether inhibition of gamma secretase with DAPT alters the regenerative response to HC loss caused by damage with an ototoxic drug, as predicted if Notch signalling regulates SC behavior. For these studies, cochlear ducts were cultured with Streptomycin for

2 days to kill HCs and were then maintained in Streptomycin-free media for one additional day. MyosinVI labeling was used to detect HCs. In contrast to the mild and locally restricted damage seen in untreated cultures, Streptomycin caused near-complete loss of HCs from all regions of the BP by 3 days in vitro, regardless of whether or not culture media contained DAPT (Fig. 5K,L). SCs had entered the cell cycle by 3 days, and like in vivo, SC division was heaviest in the neural region (data not shown). At this time, new HCs had not differentiated to the degree of expressing MyosinVI protein. However, by 8 days (2 days plus Streptomycin then 6 days minus Streptomycin), numerous MyosinVI-positive regenerated HCs were evident throughout BPs cultured in DMSO (Fig. 5M). Continuous BrdU labeling showed that some HCs regenerated in vitro were BrdU-negative and therefore formed by direct transdifferentiation, while others were BrdU-positive and therefore formed via mitosis, resembling HC regeneration in vivo.

To test how Notch activity modulates drug-induced HC regeneration, organs were first cultured for 2 days with Streptomycin followed by 1 day without Streptomycin, with DAPT (at 1, 10, or 50 μM) or DMSO (matching concentrations) present in the culture media for the whole period. In standard Notch-mediated lateral inhibition, Notch activation cell-autonomously inhibits a cell's differentiation toward the primary fate and its ability to express Notch ligands. Therefore, DAPT blockade of Notch activation should evoke increased expression of the pro-HC transcription factor, *Atoh1*, and the Notch ligand, *Delta1*. We tested this hypothesis, using ISH to detect *Atoh1* and *Delta1* transcripts.

In Streptomycin-treated organs cultured 3 days with DAPT (Fig. 6B–D), *Atoh1* transcripts were highly increased relative to DMSO controls (Fig. 6A). The degree of *Atoh1* upregulation in damaged BPs appeared to correlate directly with DAPT concentration; limited differences were seen with 1 μM DAPT (Fig. 6B), but striking effects were clear with 10 μM (Fig. 6C) or 50 μM DAPT (Fig. 6D). Similar results with DAPT were seen in the lagena (data not shown). In addition, treatment with DAPT (50 μM) caused an elevation in *Delta1* transcripts over control levels (Fig. 6E,F). In another set of experiments, we found that application of N-(R)-[2-(hydroxyaminocarbonyl)methyl]-4-methylpentanoyl-l-naphthylalanyl-l-alanine-2-aminoethyl amide (TAPI-1), a drug that inhibits a second enzyme required for Notch cleavage and activation (TNF-alpha converting enzyme, or TACE; Brou et al., 2000), to Streptomycin-treated BPs for 3 days also caused a significant upregulation in *Atoh1* transcription compared to negative control (DMSO) in a dose-dependent manner (Supplemental Fig. 2). However, in contrast to the DAPT-induced upregulation of *Atoh1* and *Delta1*, we noted no difference in *Serrate1* mRNA expression between DMSO- and DAPT-treated cultures (Fig. 6G,H), implying *Serrate1* transcription is not regulated by Notch activity in the regenerating BP.

Activation of Notch promotes transcription of *Hes* genes. We tested if inhibition of gamma secretase with DAPT leads to decreased *Hes5* transcription in the regenerating BP, using a cocktail of probes for *Hes5.1* and *Hes5.3* transcripts. In Streptomycin-damaged cochlear ducts cultured in DMSO control media for 3 days, expression of *Hes5* genes was elevated compared to quiescent organs (compare Figs. 6I and 3L,M), similar to what is seen in vivo after Gentamicin treatment (compare Figs. 6I and 3P–R). In contrast, in Streptomycin-damaged cultures treated with DAPT for 3 days, *Hes5* transcripts were markedly attenuated (compare Fig. 6I with 6J). Similar changes were seen in the lagena (data not shown).

These findings confirm that DAPT efficiently blocks Notch signalling in cultured BPs, and they serve as a positive control for DAPT experiments in BPs without Streptomycin treatment, described above. These results also show that inhibition of Notch signalling with either DAPT or TAPI-1 during drug-induced HC damage does not block the initiation of HC regeneration, as reflected by Atoh1 upregulation. Rather, inhibition of Notch induces a large and rapid upregulation in HC differentiation, suggesting that, just as during embryonic production, the

commitment of cells in the damaged BP to a HC fate is limited by Delta/Notch-mediated lateral inhibition.

Inhibition of gamma secretase leads to overproduction of HCs at the expense of SCs

Maintenance of cultures for longer periods confirmed that HCs are overproduced at the expense of SCs when Notch signalling is inhibited after HC damage. Cultures grown for 8 days (2 days with Streptomycin then 6 days without Streptomycin) with continuous DAPT showed a dramatic increase in the density of regenerated HCs compared to DMSO controls, as demonstrated by increased immunolabeling for MyosinVI (compare Fig. 7A,B and 7D,E) and Hair Cell Antigen (HCA)(Bartolami et al., 1991)(Fig. 7J,N). In this Figure, BPs treated with 50 μM DAPT or 0.5% DMSO are shown. The DAPT-induced increase in HC density was accompanied by a decrease in SC density, as shown by immunostaining for Supporting Cell Antigen, or SCA (Kruger et al., 1999)(Fig. 7C,F) and for another SC-specific antigen that is likely a precursor of β-Tectorin (Goodyear et al., 1996)(Supplemental Fig. 1). In DMSO controls (Fig. 7G–J), regenerated HCs and SCs were evenly mixed. In contrast, in DAPT-treated organs (Fig. 7K–N), regenerated HCs were numerous, tightly packed, and appeared to be in direct contact with one another, while SCs were uncommon and haphazardly distributed. Similar results were consistently seen when: 1) DAPT was used at 10, 50, or 100 μM; 2) cochlear ducts from 1 month-old chickens were used; or 3) DAPT or DMSO was added from the start of culture or after the Streptomycin exposure (data not shown).

To assess if cell death might be a cause of the reduction in SC profiles seen after DAPT treatment, we cultured BPs for shorter periods (2 days plus Streptomycin followed by either 2 days or 4 days of either 50 μM DAPT or 0.5% DMSO) and labeled them for TUNEL or activated Caspase 3. While small numbers of dying cells were detected in both DAPT and DMSO-treated samples, no qualitative difference in labeling for either cell death marker was evident (data not shown). These data suggest that that the decrease in total cell number seen after DAPT treatment is not due to increased cell death.

We noted regional variations in the response to DAPT. Proximally, DAPT caused a large increase in HC density across the entire width of the epithelium (Fig. 7D), while in middle and distal regions, DAPT caused this effect only in the neural half of the epithelium (Fig. 7E). Thus, the regions showing the strongest signs of Notch pathway activation following damage in vivo (see Fig. 3I,J,P–R) as well as the highest degree of SC division (see Fig. 3H) show the strongest effects of DAPT.

Constitutive Notch activation prevents SCs from forming new HCs

Our results show that inhibition of gamma secretase leads to attenuation of Notch activity and increased regeneration of HCs at the expense of SCs. While these findings strongly suggest that Notch signalling is required to laterally inhibit cells from differentiating into HCs after damage in the mature BP, gamma secretase cleaves a variety of signalling proteins in addition to Notch (e.g., p75, Zampieri et al., 2005), leaving open the possibility that other signalling molecules besides Notch may have this critical role.

To directly test the role of Notch in maintaining the SC phenotype after damage, we transfected SCs in cultured cochlear ducts with either one of the plasmids encoding the activating portion of the Notch receptor, NICD (*pN^{ICD}-IRES-EGFP or pCAB-NICD-IRES-EGFP*) or the *pMES* plasmid (encoding EGFP only), and examined SC behavior in each case. Cochlear ducts were cultured for 2 days with Streptomycin to kill HCs, and plasmid was transfected into some of the remaining SCs using electroporation. Cultures were maintained for two or 5 additional days, and were then fixed, immunolabeled to detect MyosinVI and GFP, and examined to determine the fate of transfected SCs.

Two days after transfection with either plasmid, MyosinVI-positive cells (HCs) were rare, since original HCs had been killed and few new HCs had been regenerated (Fig. 8A, a *pMES*-transfected BP is shown). The majority of transfected, GFP-immunoreactive (IR) cells still had SC-like morphology, with elongated cell bodies and thin cytoplasmic processes extending from the nuclear region. At 5 days post-transfection, BPs transfected with either *pMES* or pN^{ICD} contained MyosinVI-positive, regenerated HCs (Fig. 8C,F). We scored GFP-IR cells in *pMES*- or pN^{ICD}–transfected BPs at this time as either MyosinVI-positive (HC-like) or MyosinVI-negative (SC-like). In *pMES*-transfected BPs, a significantly higher percentage of GFP-IR cells were MyosinVI-positive (25.4%) than in pN^{ICD}-transfected BPs (2.0%)($p<.0001$)(Fig. 8B). We also found that GFP-IR cells that were MyosinVI-positive usually had a round or fusiform cell shape, characteristic of well differentiated HCs, while GFP-IR cells lacking MyosinVI IR were usually SC-like (Fig. 8C–H). This observation provided additional support for the use of MyosinVI labeling to define a cell as HC-like or SC-like. These data confirmed that increased Notch activity in mature avian SCs is sufficient to prevent them from generating new HCs or to instruct them to maintain a SC phenotype after HC loss. Further, these findings provide further support that the DAPT effects seen in experiments described above are due to inactivation of Notch signalling.

Moderate doses of gamma secretase inhibitor cause HC overproduction after damage without significantly affecting cell division

We next examined how cell division after damage is affected by DAPT, and how this might relate to the overproduction of HCs. Cochlear ducts were cultured with Streptomycin for 2 days followed by 6 days with DAPT (50 μM) or with 0.5% DMSO. BrdU was provided continuously. For these experiments, we used Atoh1 protein as a marker of regenerated HCs rather than MyosinVI. Atoh1 immunoreactivity is detected in differentiating HCs between 5 and 10 days post-Gentamicin, much like MyosinVI (Cafaro et al., 2007).

Organs were fixed and double-labeled for BrdU and Atoh1, and BrdU and Atoh1 labeling were quantified. We found that the number of regenerated HCs (per unit area of epithelium) was roughly two-fold higher in DAPT-treated BPs than in DMSO controls (224 ±95 s.d. for DAPT versus 116 ±21 s.d. for DMSO, $p=0.0072$)(Fig. 9A,B insets; MyosinVI labeling in parallel experiments are shown in main panels for comparison). Moreover, the DAPT specimens showed increased numbers of both BrdU-positive (Fig. 9G) and BrdU-negative HCs (Fig. 9H), although the latter effect was not statistically significant. The 50 μM DAPT did not, however, cause any significant change in the total numbers of BrdU-labeled nuclei compared to controls (Fig. 9E). These results show that 50 μM DAPT does not alter the amount of SC division, but it does cause a higher proportion of SCs and progeny of SCs to differentiate as HCs.

We also, in a separate run of the experiment, using MyosinVI as marker of new HCs, tested the effects of a still higher dose of DAPT: 100 μM. This is at or over the limit of solubility of DAPT, making it prone to precipitate out of solution and raising concerns about non-specific toxic effects. Organs were fixed as in the foregoing experiment and double-labeled for BrdU and MyosinVI, and BrdU and MyosinVI labeling were quantified. As with the 50 μM dose of DAPT, the number of new HCs was much higher in DAPT-treated BPs than in DMSO controls (112 ±34 s.d for DAPT versus 40 ±13 s.d. for DMSO, $p<0.0001$)(Fig. 9C,D). However, the BPs treated with 100 μM DAPT showed a striking decrease in the numbers of cells labeled with BrdU (Fig. 9F; $p<0.0001$). Correspondingly, very few of the HCs overproduced in response to DAPT treatment were BrdU-positive (Fig. 9I); rather, the vast majority of them were BrdU-negative (Fig. 9J). These results show that 100 μM DAPT, like 50 μM DAPT, biases SCs toward differentiation as HCs during regeneration; but, they also indicate that the very high dose of DAPT has an additional effect, not seen at lower doses, in decreasing cumulative cell division. This anti-proliferative effect could reflect a general toxicity

independent of Notch signalling. Indeed, as the next experiments show, it was not always seen even with the 100 μM DAPT dose.

Notch signalling exerts no direct influence on SC entry into the cell cycle

To examine possible effects on cell division in greater detail, we examined whether acute treatment with DAPT after Streptomycin treatment prevents SCs from entering the cell cycle in the short term. Organs were cultured for 3 days (2 days plus Streptomycin then 1 day without Streptomycin). DAPT (100 μM) or DMSO (1%) was present for the entire culture period, and BrdU was added for the last 4 hours before fixation. This early DAPT treatment allowed us to assess effects of DAPT on the initial rise in SC division, which is seen at 3 days in vitro. We detected no significant difference in the numbers of BrdU-positive nuclei between the two groups (26 ±14 s.d. for DMSO and 32 ±16 s.d. for DAPT, N=3 BPs for each group, p=0.4037) nor in the neural focus of SC division (data not shown), indicating that 100 μM DAPT did not inhibit SC recruitment into the cell cycle in this set of experiments.

We also examined whether Notch activity is required after SCs have entered the cell cycle to sustain mitotic activity. Organs were cultured for 5 days (2 days plus Streptomycin then 3 days without Streptomycin), with 100 μM DAPT or DMSO present for the final 2 days, and BrdU present for the final 24 hours. A longer BrdU pulse was provided here than for 3-day experiments, because we anticipated a decline in the number of normally dividing SCs over time (Stone et al., 1999). We noted no difference in the distribution or density of BrdU-positive nuclei between the two groups (47 ±49 for DMSO and 45 ±32 for DMSO, N=3 BPs for each group, p=0.9223), demonstrating that Notch activity is not required to maintain SC division after it is initiated.

DISCUSSION

Despite the discovery of HC regeneration in the mature avian auditory epithelium (BP) twenty years ago, the molecular cues that regulate activation of mature SCs are still largely uncharacterized. We have shown that, in the undamaged BP, Notch signalling is not responsible for inhibiting SCs from dividing or from directly transdifferentiating into HCs. Another set of signals must exert these effects. However, during regeneration after HC loss, Notch activity has a key role in limiting the number of new HCs that are generated through either mitosis or direct transdifferentiation of SCs. In the following discussion, we explain these findings in more detail and consider their implications for the logic of signals governing HC regeneration.

Changes in Notch signalling are not the trigger for regeneration

In the post-hatch avian BP, SCs are a quiescent population unless HC loss occurs. It has been hypothesized that direct contact from HCs maintains SC quiescence (Corwin et al., 1991; Cotanche, 1987). This could in theory be mediated by lateral inhibition that is dependent upon Notch ligands expressed by mature HCs (Lewis, 1991). Indeed, we show here that at least two Notch receptors (*Notch1* and *Notch2*), three ligands (*Delta1*, *Serrate1*, and *Serrate2*), and one effector (*Hes5*) are transcribed in the undamaged BP. However, expression of these Notch pathway components does not necessarily imply functional importance, and we have found that blockade of Notch signalling by DAPT in undamaged BPs is not sufficient to trigger SCs to convert into HCs or to divide. This finding is in agreement with two recent studies in other species. Ma et al. (2008) and Hori et al. (2007) showed that inhibition of gamma secretase using either DAPT or MDL does not induce HC production in undamaged lateral line neuromasts of larval zebrafish or in undamaged adult organ of Corti, respectively. In contrast, two other studies (Takebayashi et al., 2007; Yamamoto et al., 2006) showed that DAPT treatment in late embryonic organ of Corti of undamaged mice causes SCs to de-differentiate and to convert into HCs. The key to these differences may be the relative maturity of SCs. Our

study and the studies by Ma et al. (2008) and Hori et al. (2007) were performed in mature HC-epithelia, whereas the studies by Yamamoto et al. (2006) and Takebayashi et al. (2007) were performed in HC-epithelia that will not reach full maturity until 1–3 weeks later (e.g., Sher, 1971; Tannenbaum and Slepecky, 1997). Considering these studies together with our present data, we conclude that, whereas Notch signalling is needed to establish the phenotype of SCs and to limit HC production during development, other mechanisms take over the role of maintaining the quiescent SC phenotype once the sensory epithelium has matured. We discuss this point further below.

Another key finding of this study is that inhibition of Notch signalling with DAPT or TAPI-1 does not alter the degree of HC regeneration that occurs in the BP in culture. Therefore, we conclude that Notch activity is not required for SCs to transit from quiescence to a state of activation, either for renewed cell division or direct transdifferentiation, following HC damage.

Following tissue damage, Notch-mediated lateral inhibition inhibits the differentiation of hair cells formed by either mitosis or direct transdifferentiation

Although a change in Notch signalling is not the trigger for the regenerative response in the chicken BP, our data show that Notch does play a key role in directing the course of that response, once HC damage is initiated. In fact, HC loss from the post-hatch BP appears to restore the epithelium to a state resembling the developing otic epithelium as HCs are emerging: the embryonic pattern of expression of Notch pathway components is reconstituted, and Notch signalling is reactivated.

There are several distinct functions that Notch signalling might perform in the regenerative process. At early stages of development, before HC differentiation has begun, Notch activity serves in the developing inner ear to establish and/or to extend the prosensory patches (Kiernan et al., 2006; Daudet et al., 2007; Hayashi et al., 2008). We therefore considered the possibility that re-activation of Notch signalling might be necessary to initiate regeneration in the chicken BP. However, DAPT treatment before and during HC damage did not block the regenerative response, demonstrating that this is not the case.

Notch signalling also directs cell fate decisions during development via lateral inhibition. During this process, Atoh1 acts upstream of Delta1, while Notch activity inhibits expression of *Atoh1* and *Delta1* (and *Serrate2*/*Jagged2*). Cells that express Atoh1 and *Delta1* become HCs, and by activating Notch in their neighbors, they prevent their neighbors from becoming HCs and ensure that they remain as sensory progenitor cells or differentiate as SCs (Lanford et al., 2000; Millimaki et al., 2007). A similar control system evidently operates during HC regeneration in the chicken BP. Levels of Atoh1 protein increase at 1 day post-Gentamicin (Cafaro et al., 2007), followed by a rise in *Delta1* transcript levels (Stone and Rubel, 1999). Experimental blockade of Notch activity with DAPT induced a strong increase in the expression of both Atoh1 and *Delta1* in short-term cultures. In long-term cultures, DAPT caused the overproduction of HCs, via mitotic and non-mitotic mechanisms, at the expense of SCs. Overexpression of activated Notch (NICD) had the opposite effect; it maintained the SC phenotype. Collectively, our results strongly suggest that negative regulation of *Atoh1* and *Delta1* by lateral inhibition governs HC differentiation during regeneration, as it does during development, but that some factor beside reduced Notch activity triggers the initial rise of *Atoh1* expression following HC destruction.

After HC loss in the chicken BP, *Delta1* mRNA is detected in BrdU-labeled cells, suggesting that HCs formed through renewed cell division inhibit neighboring cells from differentiating as HCs (Stone and Rubel, 1999).

Notch activity is not a direct regulator of cell division in the regenerating BP

Normal regeneration in the BP involves resumption of cell division as well as switches of cell differentiation. Our data clearly show that Notch signalling governs the switches of cell differentiation. Does it also govern cell division? Given that HCs do not divide but SCs can, one might expect that activation of the Notch pathway, by blocking HC differentiation, would favor proliferation. We found, on the contrary, that expression of *Hes5*, indicative of Notch activation, was inversely correlated with BrdU labeling, suggesting that if Notch signalling has any effect on cell division, it is inhibitory. Moreover, moderate doses of DAPT, while strongly favoring HC differentiation, and thus evidently sufficient to block Notch signalling, had no significant effect on the fraction of cells entering the division cycle. In acute experiments, even the very highest dose of DAPT (100 μM) had no effect on the numbers of cells entering S-phase. However, in one set of long-term experiments involving DAPT exposure at this maximal level, we did see a strong reduction of BrdU labeling. This result was not replicated with lower DAPT levels. This reduction in BrdU labeling may be a Notch-independent toxic side-effect of high-dose DAPT. Alternatively, it may reflect an actual long-term reduction in SC division that occurred because the high-dose DAPT triggered a massive conversion of SCs into HCs by direct transdifferentiation and depletion of SCs. However, this is hard to reconcile with the rest of the data. The more likely interpretation seems to be that cell division during regeneration is controlled by some influence other than Notch signalling.

Two types of signals control the behavior of supporting cells: one delivered via Notch, the other independent of Notch

If Notch activity is not required to keep SCs quiescent in the undamaged state or to regulate their ability to divide following HC damage, then what are the signals that regulate these important SC behaviors? Our working hypothesis is that HCs deliver two types of inhibitory signals to their neighbors. The first type, the Quiescence (Q) signal, is independent of Notch, functions during quiescence and regeneration, and inhibits SCs from directly transdifferentiating into HCs and from dividing. The second signal, the Notch (N) signal, is necessary for normal embryonic development and during regeneration, but it does not maintain quiescence or directly control cell division. Rather, its function after HC damage is to limit, via lateral inhibition, the proportion of SCs and SC progeny that differentiate into HCs. A corollary of our two-signal hypothesis is that Q and N signals act in parallel to restrict HC differentiation. Depending on the relative timing and intensity of their actions, one signal or the other might predominate. This could explain differences that we saw in regenerative behavior and in the response to DAPT of SCs on the neural and abneural sides of the BP.

What is the molecular basis of the Q signal? One suggestion is that it might take the form of a cadherin-mediated interaction between HCs and their neighbors (Warchol, 2002). Other cell-surface signalling molecules, such as Ephrins and Eph family members, are also candidates for such a role, as are soluble factors, such as those of the Wnt, FGF, and BMP families. The nature of the signal(s) that initiate regeneration and control the proliferation of SCs is a central problem for future research.

Supplementary Material

Refer to Web version on PubMed Central for supplementary material.

Acknowledgements

We thank Jane Johnson and Guy Richardson for antibodies, Catherine Krull, Fernando Giraldez, Cliff Tabin, and Domingos Henrique for plasmids, and Andrew Forge, Jonathan Bird, and Eva Ma for comments on the manuscript. We also thank Edwin Rubel for sharing facilities, Glen MacDonald for assistance with microscopy, and Karina Cramer for assisting to develop the electroporation technique. Finally, we would like to thank James Garlick and Ling Tong

for technical assistance with electroporation and in situ hybridization. This work was supported by the Hearing Regeneration Initiative, NIH DC03696, NIH DC03829, NIH DC04661 and NIH HD002274, Cancer Research UK, and Deafness Research UK.

References

Adam J, Myat A, LeRoux I, Eddison M, Henrique D, Ish-Horowicz D, Lewis J. Cell fate choices and the expression of *Notch*, *Delta*, and *Serrate* homologs in the chick inner ear: Parallels with Drosophila sense-organ development. Development 1998;125:4645–4654. [PubMed: 9806914]

Adler HJ, Raphael Y. New hair cells arise from supporting cell conversion in the acoustically damaged chick inner ear. Neurosci Lett 1996;205:17–20. [PubMed: 8867010]

Artavanis-Tsakonas S, Matsuno K, Fortini ME. Notch signalling. Science 1995;268:225–32. [PubMed: 7716513]

Bartolami S, Goodyear R, Richardson G. Appearance and distribution of the 275 kD hair-cell antigen during development of the avian inner ear. J Comp Neurol 1991;314:777–88. [PubMed: 1816275]

Bermingham NA, Hassan BA, Price SD, Vollrath MA, Ben-Arie N, Eatock RA, Bellen HJ, Lysakowski A, Zoghbi HY. *Math1*: an essential gene for the generation of inner ear hair cells. Science 1999;284:1837–1841. [PubMed: 10364557]

Brooker R, Hozumi K, Lewis J. Notch ligands with contrasting functions: Jagged1 and Delta1 in the mouse inner ear. Development 2006;133:1277–86. [PubMed: 16495313]

Brou C, Logeat F, Gupta N, Bessia C, LeBail O, Doedens JR, Cumano A, Roux P, Black RA, Israël A. A novel proteolytic cleavage involved in Notch signaling: the role of the disintegrin-metalloprotease TACE. Mol Cell 2007;5:207–16. [PubMed: 10882063]

Cafaro J, Lee GS, Stone JS. Atoh1 expression defines activated progenitors as well as differentiating hair cells during avian hair cell regeneration. Dev Dyn 2007;236:156–170. [PubMed: 17096404]

Colebrooke RE, Chan PM, Lynch PJ, Mooslehner K, Emson PC. Differential gene expression in the striatum of mice with very low expression of the *vesicular monoamine transporter type 2* gene. Brain Res 2007;1152:10–6. [PubMed: 17433807]

Corwin JT, Cotanche DA. Regeneration of sensory hair cells after acoustic trauma. Science 1988;240:1772–74. [PubMed: 3381100]

Corwin JT, Jones JE, Katayama A, Kelley MW, Warchol ME. Hair cell regeneration: the identities of progenitor cells, potential triggers and instructive cues. Ciba Found Symp 1991;160:103–20. [PubMed: 1752159]discussion 120–30

Cotanche DA. Regeneration of hair cell stereociliary bundles in the chick cochlea following severe acoustic trauma. Hear Res 1987;30:181–94. [PubMed: 3680064]

Crosnier C, Vargesson N, Gschmeissner S, Ariza-McNaughton L, Morrison A, Lewis J. Delta-Notch signalling controls commitment to a secretory fate in the zebrafish intestine. Development 2005;132:1093–104. [PubMed: 15689380]

Crosnier C, Stamataki D, Lewis J. Organizing cell renewal in the intestine: stem cells, signals and combinatorial control. Nat Rev Genet 2006;7:349–59. [PubMed: 16619050]

Daudet N, Lewis J. Two contrasting roles for Notch activity in chick inner ear development: specification of prosensory patches and lateral inhibition of hair-cell differentiation. Development 2005;132:541–51. [PubMed: 15634704]

Daudet N, Ariza-McNaughton L, Lewis J. Notch signalling is needed to maintain, but not to initiate, the formation of prosensory patches in the chick inner ear. Development 2007;134:2369–2378. [PubMed: 17537801]

Dovey HF, John V, Anderson JP, Chen LZ, de Saint Andrieu P, Fang LY, Freedman SB, Folmer B, Goldbach E, et al. Functional gamma-secretase inhibitors reduce beta-amyloid peptide levels in brain. J Neurochem 2001;76:173–81. [PubMed: 11145990]

Ginzberg RD, Gilula NB. Modulation of cell junctions during differentiation of the chicken otocyst sensory epithelium. Dev Biol 1979;68(1):110–29. [PubMed: 437313]

Goodyear R, Killick R, Legan PK, Richardson GP. Distribution of *beta-tectorin* mRNA in the early posthatch and developing avian inner ear. Hear Res 1996;96:167–78. [PubMed: 8817316]

Haltiwanger RS. Regulation of signal transduction pathways in development by glycosylation. Curr Opin Struct Biol 2002;12:593–8. [PubMed: 12464310]

Hashino E, Salvi R. Changing patterns of DNA replication in the noise-damaged chick cochlea. J Cell Science 1993;105:23–31. [PubMed: 8360276]

Hasson T, Gillespie PG, Garcia JA, MacDonald RB, Zhao Y, Yee AG, Mooseker MS, Corey DP. Unconventional myosins in inner-ear sensory epithelia. J Cell Biol 1997;137:1287–307. [PubMed: 9182663]

Hayashi T, Kokubo H, Hartman BH, Ray CA, Reh TA, Bermingham-McDonogh O. Hesr1 and Hesr2 may act as early effectors of Notch signalling in the developing cochlea. Dev Biol 2008;316(1):87–99. [PubMed: 18291358]

Henrique D, Adam J, Myat A, Chitnis A, Lewis J, Ish-Horowitz D. Expression of a *Delta* homolog in prospective neurons in the chick. Nature 1995;375:787–790. [PubMed: 7596411]

Hori R, Nakagawa T, Sakamoto T, Matsuoka Y, Takebayashi S, Ito J. Pharmacological inhibition of Notch signalling in the mature guinea pig cochlea. Neuroreport 2007;18(18):1911–4. [PubMed: 18007185]

Kageyama R, Ohtsuka T, Hatakeyama J, Ohsawa R. Roles of bHLH genes in neural stem cell differentiation. Exp Cell Res 2005;306:343–8. [PubMed: 15925590]

Katayama A, Corwin JT. Cell production in the chicken cochlea. J Comp Neurol 1989;281(1):129–35. [PubMed: 2925897]

Kelley MW. Regulation of cell fate in the sensory epithelia of the inner ear. Nat Rev Neurosci 2006;7 (11):837–49. [PubMed: 17053809]Review. Erratum in: Nat Rev Neurosci. 2007 Mar;8(3):239

Kiernan AE, Cordes R, Kopan R, Gossler A, Gridley T. The Notch ligands DLL1 and JAG2 act synergistically to regulate hair cell development in the mammalian inner ear. Development 2005;132 (19):4353–62. [PubMed: 16141228]

Kiernan AE, Xu J, Gridley T. The Notch ligand JAG1 is required for sensory progenitor development in the mammalian inner ear. PLoS Genet 2006;2(1):e4. [PubMed: 16410827]

Kruger RP, Goodyear RJ, Legan PK, Warchol ME, Raphael Y, Cotanche DA, Richardson GP. The supporting-cell antigen: a receptor-like protein tyrosine phosphatase expressed in the sensory epithelia of the avian inner ear. J Neurosci 1999;19:4815–27. [PubMed: 10366616]

Kuroda K, Han H, Tani S, Tanigaki K, Tun T, Furukawa T, Taniguchi Y, Kurooka H, Hamada Y, Toyokuni S, Honjo T. Regulation of marginal zone B cell development by MINT, a suppressor of Notch/RBP-J signalling pathway. Immunity 2003;18:301–12. [PubMed: 12594956]

Lanford PJ, Lan Y, Jiang R, Lindsell C, Weinmaster G, Gridley T, Kelley MW. Notch signalling pathway mediates hair cell development in mammalian cochlea. Nat Genet 1999;21:289–92. [PubMed: 10080181]

Lanford PJ, Shailam R, Norton CR, Gridley T, Kelley MW. Expression of *Math1* and *HES5* in the cochleae of wildtype and Jag2 mutant mice. J Assoc Res Otolaryngol 2000;1:161–71. [PubMed: 11545143]

Lewis, J. Rules for the production of sensory cells. In: Bock, G.; Whelan, J., editors. Regeneration of Vertebrate Sensory Receptor Cells. Wiley and Jones; New York: p. 103-119.

Lewis J. Neurogenic genes and vertebrate neurogenesis. Curr Opin Neurobiol 1996;6:3–10. [PubMed: 8794055]

Lewis J. Notch signalling and the control of cell fate choices in vertebrates. Semin Cell Dev Biol 1998;9:583–9. [PubMed: 9892564]

Ma EY, Rubel EW, Raible DW. Notch signalling regulates the extent of hair cell regeneration in the zebrafish lateral line. J Neurosci 2008;28(9):2261–73. [PubMed: 18305259]

Millimaki BB, Sweet EM, Dhason MS, Riley BB. Zebrafish *atoh1* genes: classic proneural activity in the inner ear and regulation by Fgf and Notch. Development 2007;134:295–305. [PubMed: 17166920]

Morrison AC, Hodgetts Gossler A, Hrabé de Angelis M, Lewis J. Expression of *Delta1* and *Serrate1 (Jagged1*) in the mouse inner ear. Mech Dev 1999;84:169–72. [PubMed: 10473135]

Oesterle EC, Rubel EW. Postnatal production of supporting cells in the chick cochlea. Hear Res 1993;66:213–24. [PubMed: 8509311]

Pfaffl MW. A new mathematical model for relative quantification in real-time RT-PCR. Nucleic Acids Res 2001;29:e45. [PubMed: 11328886]

Raphael Y. Evidence for supporting cell mitosis in response to acoustic trauma in the avian inner ear. J Neurocytol 1992;21:663–71. [PubMed: 1403011]

Roberson DW, Kreig S, Rubel EW. Light microscopic evidence that direct transdifferentiation gives rise to new hair cells in regenerating avian auditory epithelium. Aud Neuroscience 1996;2:195–205.

Roberson DW, Alosi JA, Cotanche DA. Direct transdifferentiation gives rise to the earliest new hair cells in regenerating avian auditory epithelium. J Neurosci Res 2004;78:461–71. [PubMed: 15372572]

Ryals BM, Rubel EW. Hair cell regeneration after acoustic trauma in adult *Cortunix* quail. Science 1988;240:1774–76. [PubMed: 3381101]

Selkoe D, Kopan R. Notch and Presenilin: regulated intramembrane proteolysis links development and degeneration. Annu Rev Neurosci 2003;26:565–97. [PubMed: 12730322]

Sher A. The embryonic and postnatal development of the inner ear of the mouse. Acta Otolaryngol Suppl 1971;285:1–77. [PubMed: 4334052]

Stone JS, Cotanche DA. Identification of the timing of S phase and the patterns of cell proliferation during hair cell regeneration in the chick cochlea. J Comp Neurol 1994;341:50–67. [PubMed: 8006223]

Stone JS, Leano SG, Baker LP, Rubel EW. Hair cell differentiation in chick cochlear epithelium after aminoglycoside toxicity: in vivo and in vitro observations. J Neurosci 1996;16:6157–74. [PubMed: 8815898]

Stone JS, Rubel EW. *Delta1* expression during avian hair cell regeneration. Development 1999;126:961–73. [PubMed: 9927597]

Stone JS, Choi YS, Woolley SM, Yamashita H, Rubel EW. Progenitor cell cycling during hair cell regeneration in the vestibular and auditory epithelia of the chick. J Neurocytol 1999;28:863–76. [PubMed: 10900090]

Stone JS, Rubel EW. Temporal, spatial, and morphologic features of hair cell regeneration in the avian basilar papilla. J Comp Neurol 2000;417:1–16. [PubMed: 10660884]

Stone JS, Cotanche DA. Hair cell regeneration in the avian auditory epithelium. Int J Dev Biol 2007;51:633–47. [PubMed: 17891722]

Takebayashi S, Yamamoto N, Yabe D, Fukuda H, Kojima K, Ito J, Honjo T. Multiple roles of Notch signalling in cochlear development. Dev Biol 2007;307(1):165–78. [PubMed: 17531970]

Tannenbaum J, Slepecky NB. Localization of microtubules containing posttranslationally modified tubulin in cochlear epithelial cells during development. Cell Motil Cytoskeleton 1997;38(2):146–62. [PubMed: 9331219]

van Es JH, van Gijn ME, Riccio O, van den Born M, Vooijs M, Begthel H, Cozijnsen M, Robine S, Winton DJ, Radtke F, et al. Notch/gamma-secretase inhibition turns proliferative cells in intestinal crypts and adenomas into goblet cells. Nature 2005;435:959–963. [PubMed: 15959515]

Warchol ME. Cell density and N-cadherin interactions regulate cell proliferation in the sensory epithelia of the inner ear. J Neurosci 2002;22:2607–2616. [PubMed: 11923426]

Woods C, Montcouquiol M, Kelley MW. Math1 regulates development of the sensory epithelium in the mammalian cochlea. Nat Neurosci 2004;7(12):1310–8. [PubMed: 15543141]

Yamamoto N, Tanigaki K, Tsuji M, Yabe D, Ito J, Honjo T. Inhibition of Notch/RBP-J signalling induces hair cell formation in neonate mouse cochleas. J Mol Med 2006;84(1):37–45. [PubMed: 16283144]

Yoon K, Gaiano N. Notch signalling in the mammalian central nervous system: insights from mouse mutants. Nat Neurosci 2005;8:709–15. [PubMed: 15917835]

Zampieri N, Xu C, Neubert TA, Chao MV. Cleavage of p75 neurotrophin receptor by -secretase and -secretase requires specific receptor domains. J Biol Chem 2005;80:14563–71. [PubMed: 15701642]

Zheng JL, Shou J, Guillemot F, Kageyama R, Gao WQ. Hes1 is a negative regulator of inner ear hair cell differentiation. Development 2000;127:4551–60. [PubMed: 11023859]

Zine A, de Ribaupierre F. Notch/Notch ligands and Math1 expression patterns in the organ of Corti of wild-type and Hes1 and Hes5 mutant mice. Hear Res 2002;170:22–31. [PubMed: 12208538]

Zine A, Aubert A, Qiu J, Therianos S, Guillemot F, Kageyama R, de Ribaupierre F. Hes1 and Hes5 activities are required for the normal development of the hair cells in the mammalian inner ear. J Neurosci 2001;21(13):4712–20. [PubMed: 11425898]

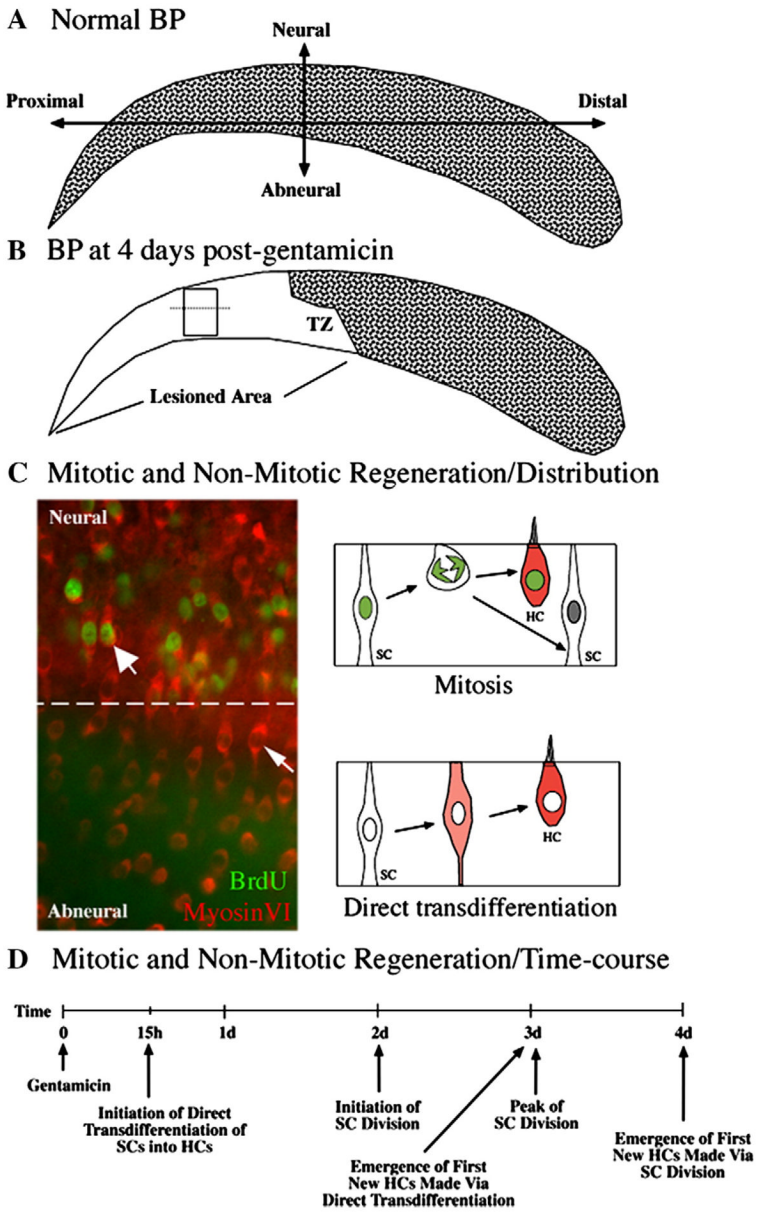

Figure 1. HC regeneration in the avian BP after short Gentamicin treatment

A. HCs (stippling) are distributed throughout the undamaged BP. The neural side of the BP is indicated and overlies the cochlear ganglion. **B.** HCs are missing from the proximal BP at 4 days post-Gentamicin (no stippling). The zone of transition (TZ) between damaged and undamaged epithelium is indicated. **C.** Immunolabeling for MyosinVI (red) and BrdU (green) in the damaged BP, in the region shown in the rectangular box in B. The dotted line separates neural and abneural regions. BrdU-positive cells are densest in the neural (upper) region, although regenerated HCs (MyosinVI-positive) are distributed throughout the neural-abneural axis. HCs regenerated via mitosis have BrdU-labeled nuclei (thick arrow) and are densest in the neural side, while HCs regenerated via direct transdifferentiation have BrdU-negative nuclei (thin arrow) and are most common in the abneural side. The two mechanisms of HC regeneration are diagrammed on the right side of C. **D**. The time-course of mitotic and non-mitotic regeneration is outlined. d=days; h=hours.

A

$2^{-\Delta Ct}$

Gene name	Control		1 day post-Gentamicin		4 days post-Gentamicin	
	Mean	sd	Mean	sd	Mean	sd
β-Tect	1.0296	0.2752	1.0228	0.4961	1.7513	0.7467
MyoVI	0.0235	0.0055	0.0315	0.0061	0.0340	0.0057
Notch1	0.0285	0.0017	0.0166	0.0059	0.0494	0.0096
Notch2	0.0415	0.0188	0.0054	0.0026	0.0451	0.0172
Ser1	0.0214	0.0124	0.0062	0.0064	0.0409	0.0253
Ser2	0.0037	0.0027	0.0053	0.0056	0.0033	0.0010
Delta1	0.0008	0.0004	0.0004	0.0003	0.0026	0.0010
Atoh1	0.0010	0.0002	0.0052	0.0005	0.0224	0.0021
Hes5	0.0074	0.0010	0.0024	0.0010	0.0153	0.0028
Hes6	0.0002	0.0000	0.0004	0.0004	0.0050	0.0010
MINT	0.0021	0.0005	0.0045	0.0017	0.0052	0.0029
Lnfg	0.0006	0.0001	0.0008	0.0002	0.0029	0.0002

B

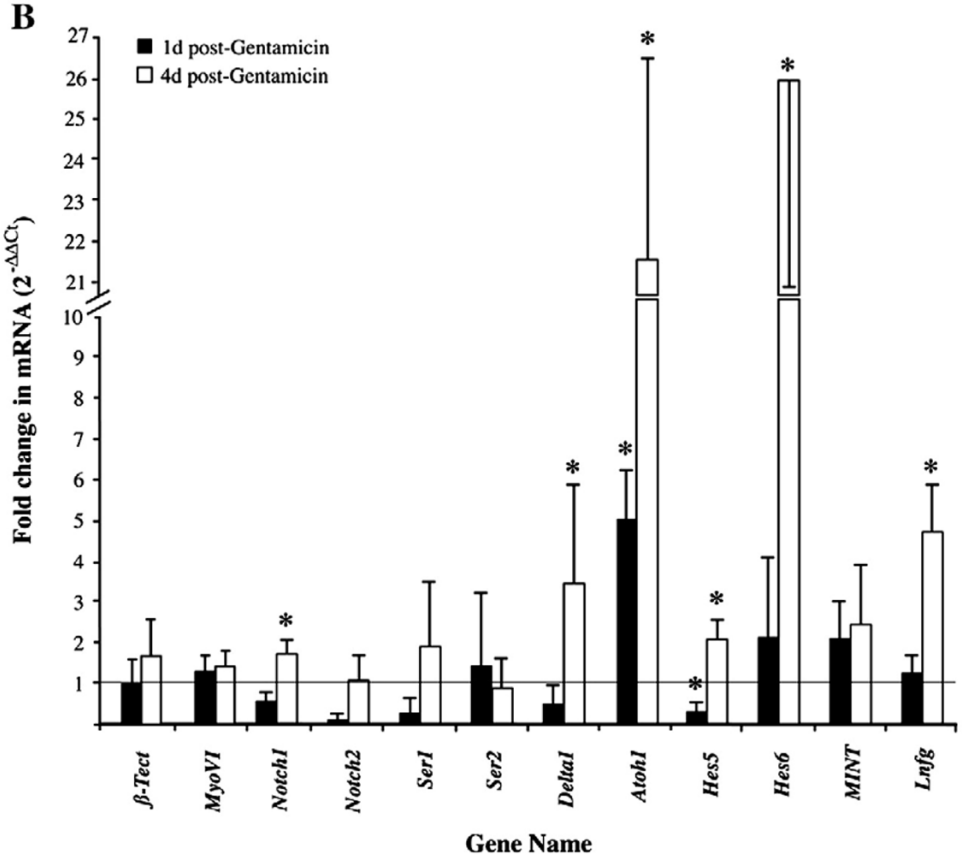

Figure 2. Differential expressison of Notch pathway genes in the quiescent and regenerating chicken BP

Transcripts were quantified by qRTPCR, and data were analyzed using the $2^{-\Delta\Delta Ct}$ method. **A.** The table shows mRNA expression for each target gene relative to *β-Actin* ($2^{-\Delta Ct}$). Data were averaged across 3 samples for each condition; standard deviations (sd) are shown. Genes showing significant differences in each treatment group compared to controls (ANOVA; $p \leq 0.05$) are highlighted in yellow. **B.** The graph shows average fold changes in mRNA between each treatment group and the control group ($2^{-\Delta\Delta Ct}$), with error bars representing standard deviations. A value of 1 (line) represents no difference from control. Asterisks indicate genes

with significant differences in $2^{-\Delta Ct}$ between each treatment group compared to controls (ANOVA; $p \leq 0.05$).

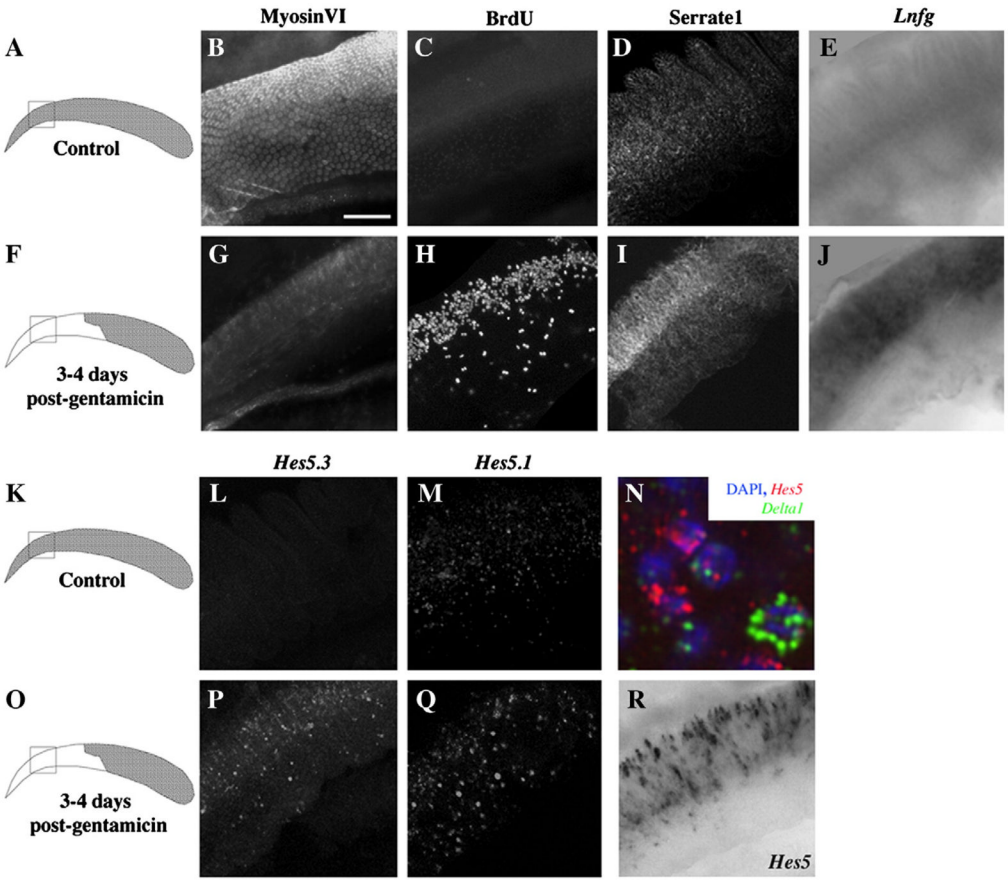

Figure 3. Localization of Notch-related gene expression in the quiescent and regenerating chicken BP

All panels except the drawings in the left column show epifluorescent or brightfield images of the proximal whole-mounted BP. The box in each drawing shows the region from which images were taken for all panels in that row. Neural is toward the top, and proximal is toward the left. Panels B–E and L–M show control, undamaged BPs, and panels G–J, N, and P–R show BPs at 3–4 days post-Gentamicin. **B,G**. Immunolabeling for MyosinVI in control (B) and damaged (G) BPs. **C,H**. Fluorescent BrdU labeling (2-hour pulse/fix) in undamaged BP (C) and in BP after damage (H). **D,I.** Serrate1 immunofluorescence in control BP (D) and in BP after damage (I). In damaged BP, immunolabeling for Serrate1 increased after damage in the neural half of BP (**I**). *In situ* hybridization (ISH) shows low levels or no of expression of *Lnfg* (**E**) and *Hes5.3* (**L**), and some *Hes5.1* expression (**M**), in control BP. ISH shows upregulated expression of *Lnfg* (**J**), *Hes5.3* (**P**), and *Hes5.1 (***Q**) in neural BP after damage. Simultaneous labeling with probes for *Hes5.1* and *Hes5.3* shows *Hes5* upregulation in neural BP (**R). N**. Triple labeling of *Hes5's* (red), *Delta1* (green), and DAPI (blue) shows little co-localization of *Hes5* and *Delta1*. Scale bar = 60 μm for all panels, except in N, where scale bar = 6 μm.

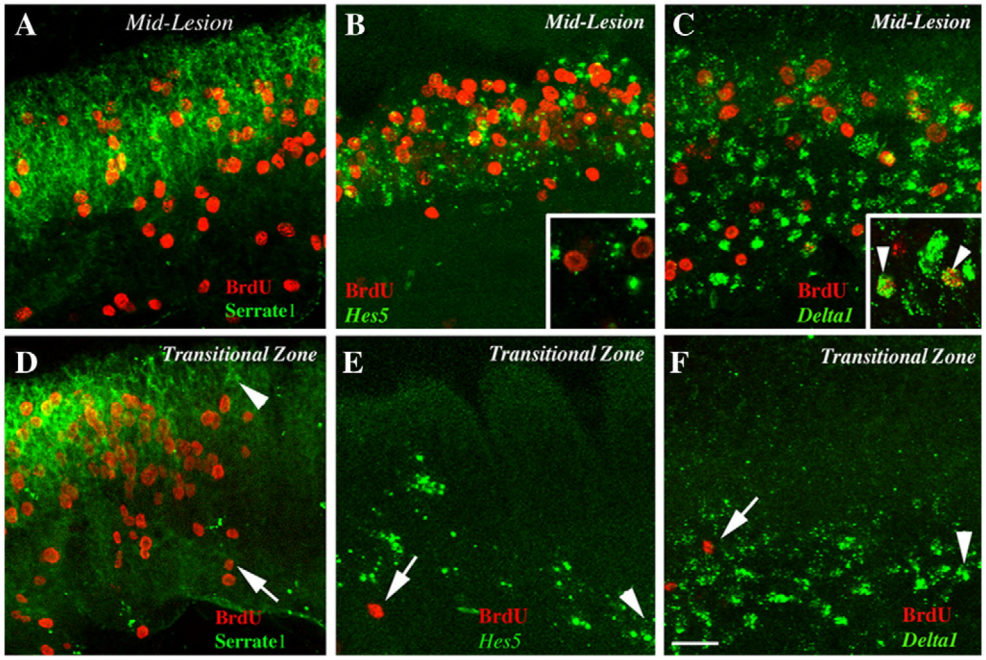

Figure 4. Spatial relationships of Serrate1, *Hes5*, and *Delta1* expression and BrdU labeling

All panels show whole-mounted BPs at 4 days post-Gentamicin. The distal end is toward the right, and the neural edge is toward the top. In all panels, BrdU labeling (red) is shown after a 2-hour BrdU pulse followed by immediate fixation. Panels A and D also show Serrate1 protein labeling (green). B and E also show *Hes5* mRNA labeling (green). C and F also show *Delta1* mRNA labeling (green). A–C. Images from the middle of the damaged region. D–F. Images from the transitional zone. Insets in B and C show larger magnifications of labeling; arrowheads in C inset show cells double-labeled for BrdU and *Delta1*. In panels D–F, the apical-most labeling for ISH or BrdU is indicated by an arrowhead or an arrow, respectively. Scale bar = 15 μm for A–F and 7 μm for insets in B and C.

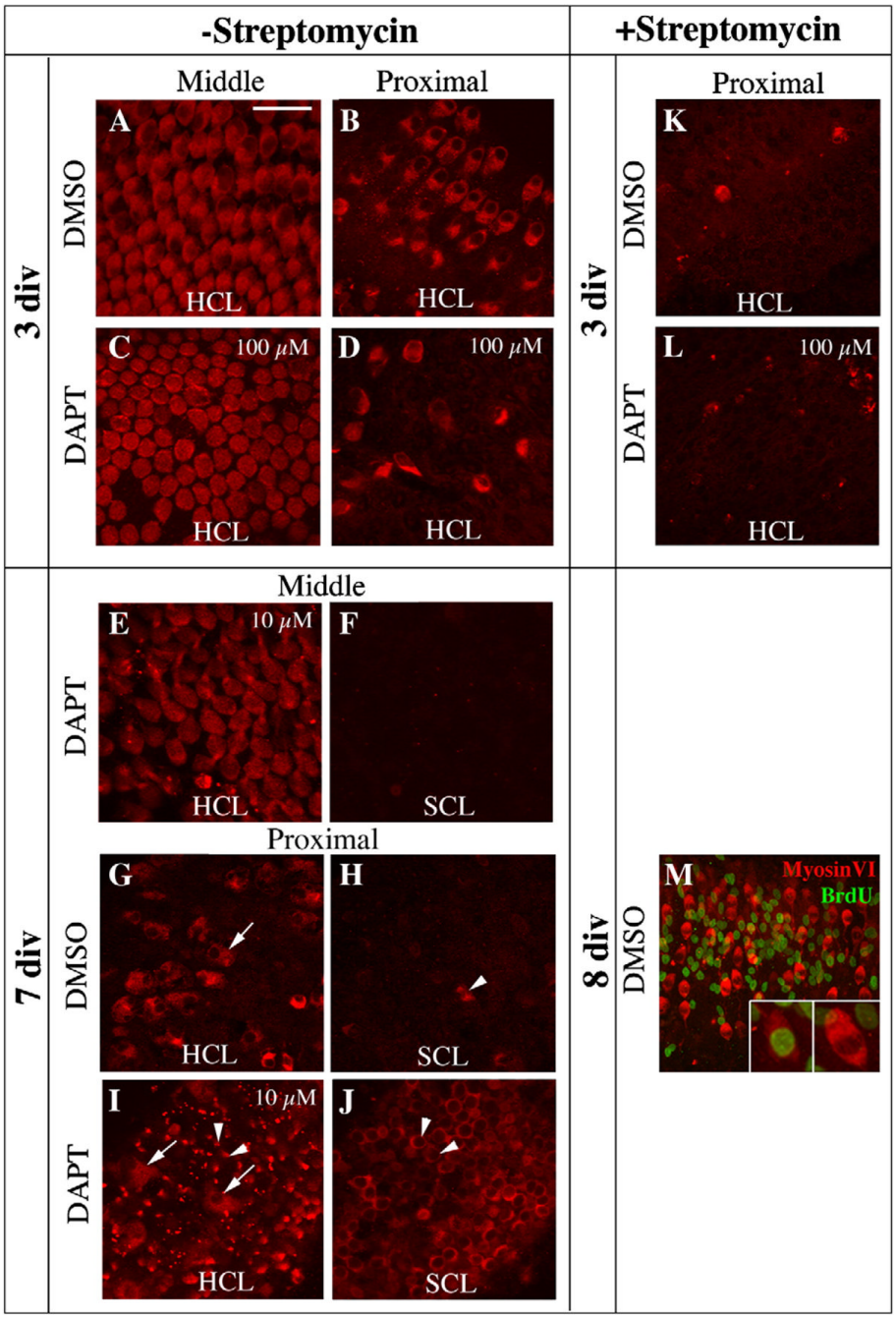

Figure 5. In vitro DAPT treatment does not alter HC regeneration in undamaged epithelium

Panels A–L show Z-projected confocal stacks of MyosinVI labeling (red) in the middle or proximal region of the BP (see Fig. 1), after DMSO or DAPT treatment. The plane of focus, in the more lumenal HC nuclear layer (HCL) or in the deeper region, the SC nuclear layer (SCL), is indicated. Concentrations for DAPT are 100 μM for C,D,L and 10 μM for E,F,I,J. DMSO concentrations were matched for comparisons. Panels **A**–**D** show BPs cultured for 3 days without Streptomycin. The degree of spontaneous HC loss is lower in the middle region (**A,C**) than in the proximal region (**B,D**). DAPT caused no increase in HC death in either region compared to DMSO (compare A with C, and B with D). Panels **E**–**J** show BPs cultured for 7 days without Streptomycin. The same field is shown in E and F, in G and H, and in I and J,

with E,G, and I focused on the HCL and F,H, and J focused on the SCL. DAPT did not promote new HC production in the middle region (**E,F**), which retained most original HCs. However, in the proximal region, where significantly fewer original HCs survived, DAPT caused increased HC regeneration (**I,J**) compared to DMSO controls (**G,H**). Arrows in G and I point to surviving original HCs (large cells, nuclei in HCL). Arrowheads in H–J point to newly regenerated HCs whose necks protrude into the HCL (I) and whose nuclei reside in the SCL (H,J) **K,L**. In BPs maintained for 3 in vitro with Streptomycin, similar levels of drug-induced HC loss were seen in BPs treated with DMSO or DAPT. **M**. BPs cultured for 8 days (2 days plus Streptomycin then 6 days minus Streptomycin, with DMSO and BrdU present for the last 6 days) have numerous MyosinVI-positive regenerated HCs (red). BrdU labeling (green) indicates new cells that were formed by mitosis. Insets show a BrdU-positive cell generated though mitosis (left) and a BrdU-negative cell regenerated via direct transdifferentiation (right). Scale bar (in A) = 20 μm for A–J, 40 μm for M, and 10 μm for M insets.

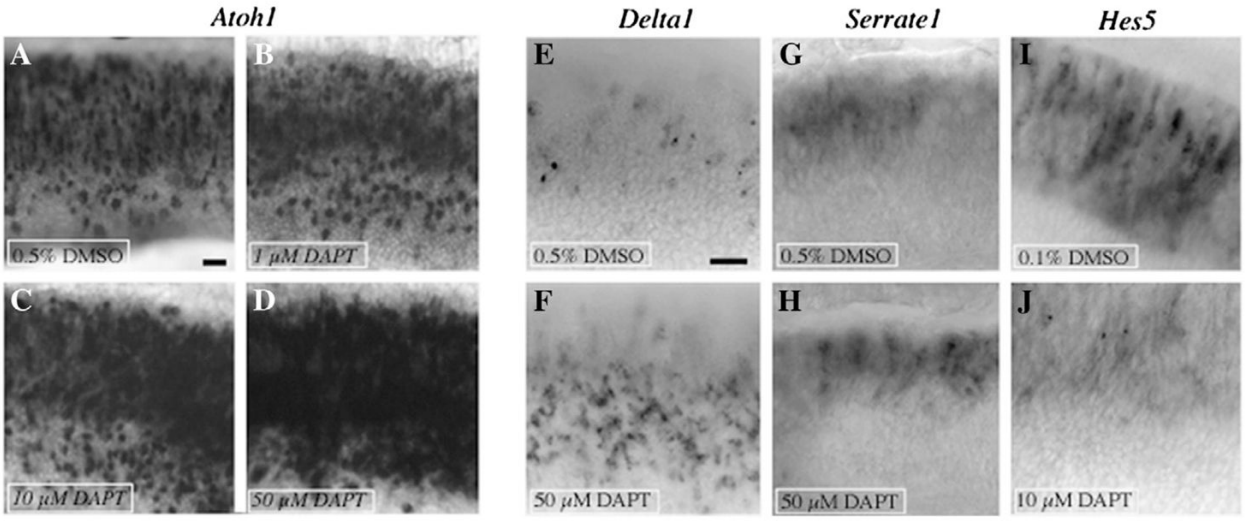

Figure 6. In vitro DAPT treatment alters transcription of Notch-related genes in drug-damaged BPs

Images were taken from BPs cultured for 3 days (2 days plus Streptomycin then 1 day minus Streptomycin), with either DMSO or DAPT present for the entire culture period. Images show the middle region, with the neural half toward the top, and the distal end toward the right. **A–D**. ISH for *Atoh1* in BPs treated with 0.5% DMSO (A), 1 μM DAPT (B), 10 μM DAPT (C), or 50 μM DAPT (D). **E,F.** ISH for *Delta1* in BPs treated with 0.5% DMSO (E) or 50 μM DAPT (F). **G,H**. ISH for *Serrate1* in BPs treated with 0.5% DMSO (G) or 50 μM DAPT (H). **I,J.** ISH for *Hes5's* in BPs treated with 0.1% DMSO (I) or 10 μM DAPT (J). Scale bar in A= 15 μm (applies to A–D), and scale bar in E = 15 μm (applies to E–J).

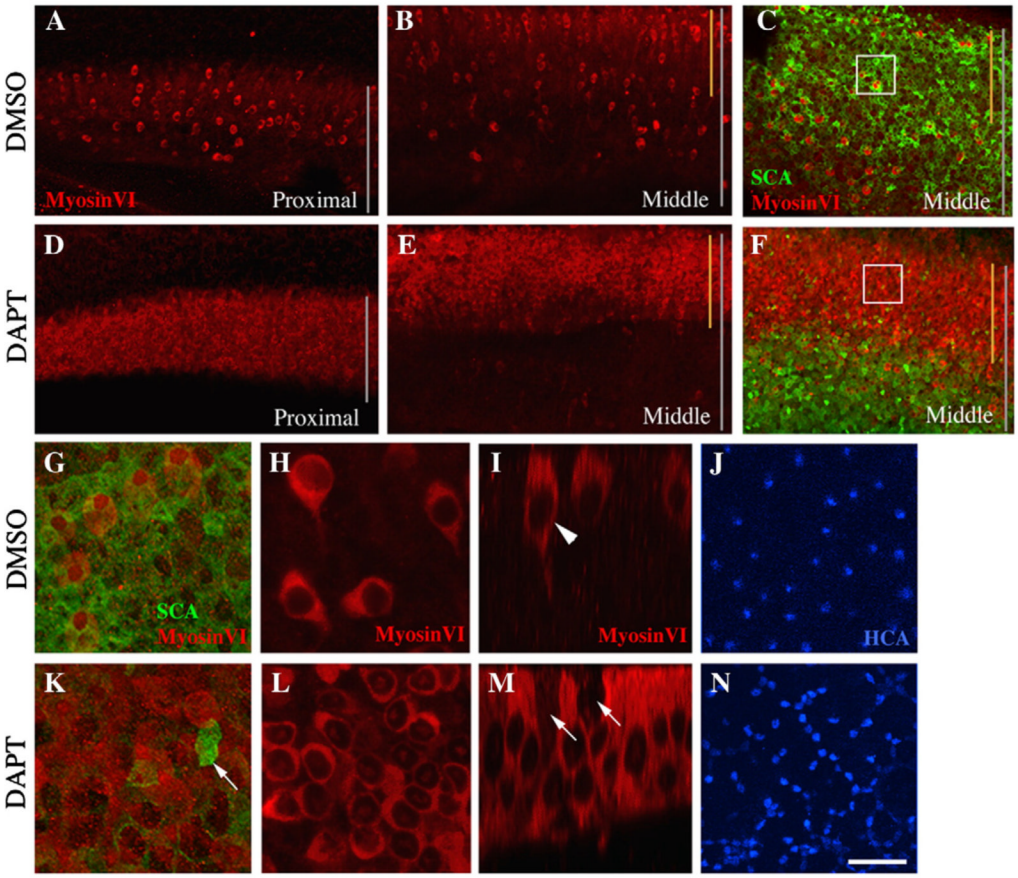

Figure 7. DAPT treatment triggers overproduction of auditory HCs by direct transdifferentiation following drug-induced HC loss

All images except I and M are Z-projections of the BP after DMSO (0.5%; **A–C,G–J**) or DAPT (50 μM; **D–F,K–N**) treatment for 6 days after an initial 2-day Streptomycin treatment. In these images, the neural edge is toward the top, and the distal end is toward the right. In **A–F**, vertical gray lines indicate the entire width of the BP, and vertical yellow lines show the extent of the neural region. **A,B.** MyosinVI labeling shows the pattern of HC regeneration in DMSO-treated BPs, in proximal (A) and middle (B) regions. **D,E**. MyosinVI labeling reveals HC overproduction in DAPT-treated BPs in proximal (D) and middle (E) regions. **C,F.** SCA labeling (green) in the middle region reveals the distribution of differentiated SCs after DMSO (C) or DAPT (F) treatment; MyosinVI labeling (red) demonstrates HC overproduction in the neural half. **G,K**. Higher-magnification taken near the boxed regions in C and F. Arrow in K points to an SCA-positive SC(s). **H,I,L,M.** MyosinVI labeling is shown in whole-mounts (H,L) or vertical slices (I,M) through the neural half of DMSO- (H,I) or DAPT- (L,M) treated BPs. Arrowhead in I points to a regenerated HC; arrows in M point to MyosinVI-negative cells (presumed SCs). **J,N.** HCA labeling in the middle-neural region of DMSO- (J) or DAPT- (N) treated BPs is shown. Scale bar = 50 μm for A–F, 10 μm for G–N.

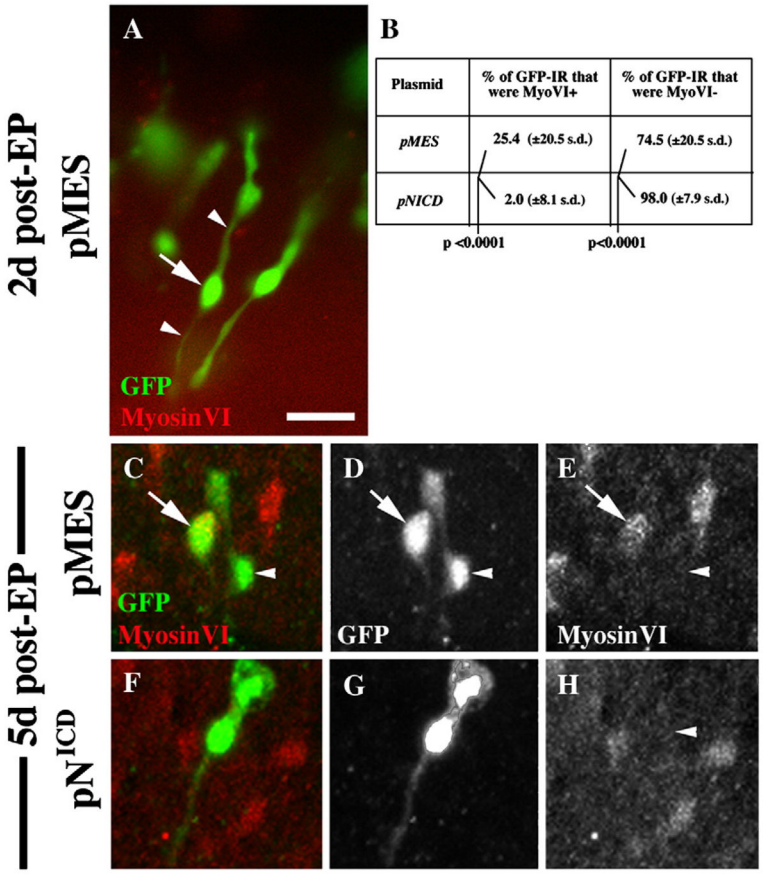

Figure 8. Overexpression of NICD prevents SCs from directly converting into HCs after damage

This figure shows representative GFP-positive cells (green) in brightest point Z-projection images from BPs at 2 days (A) or 5 days (C–H) after transfection of negative control plasmid (*pMES*) or pN^{ICD}. Counterlabeling for MyosinVI is shown in red. **A.** GFP-positive cells at 2 days after transfection with *pMES* have SC-like features (long cytoplasmic processes [arrowheads] that are MyosinVI-negative; arrow points to nucleus). **B.** Quantitative data from cultures at 5 days post-transfection (C–H). **C–E**. GFP-positive cells at 5 days after transfection with *pMES* have either a HC-like morphology (MyosinVI-positive and fusiform or round) or a SC-like morphology. **F–H**. The vast majority of GFP-positive cells at 5 days after transfection with pN^{ICD} have a SC-like morphology. Images in C and F are shown in separate channels in D,E and G,H, respectively. Scale bar = 20 μm.

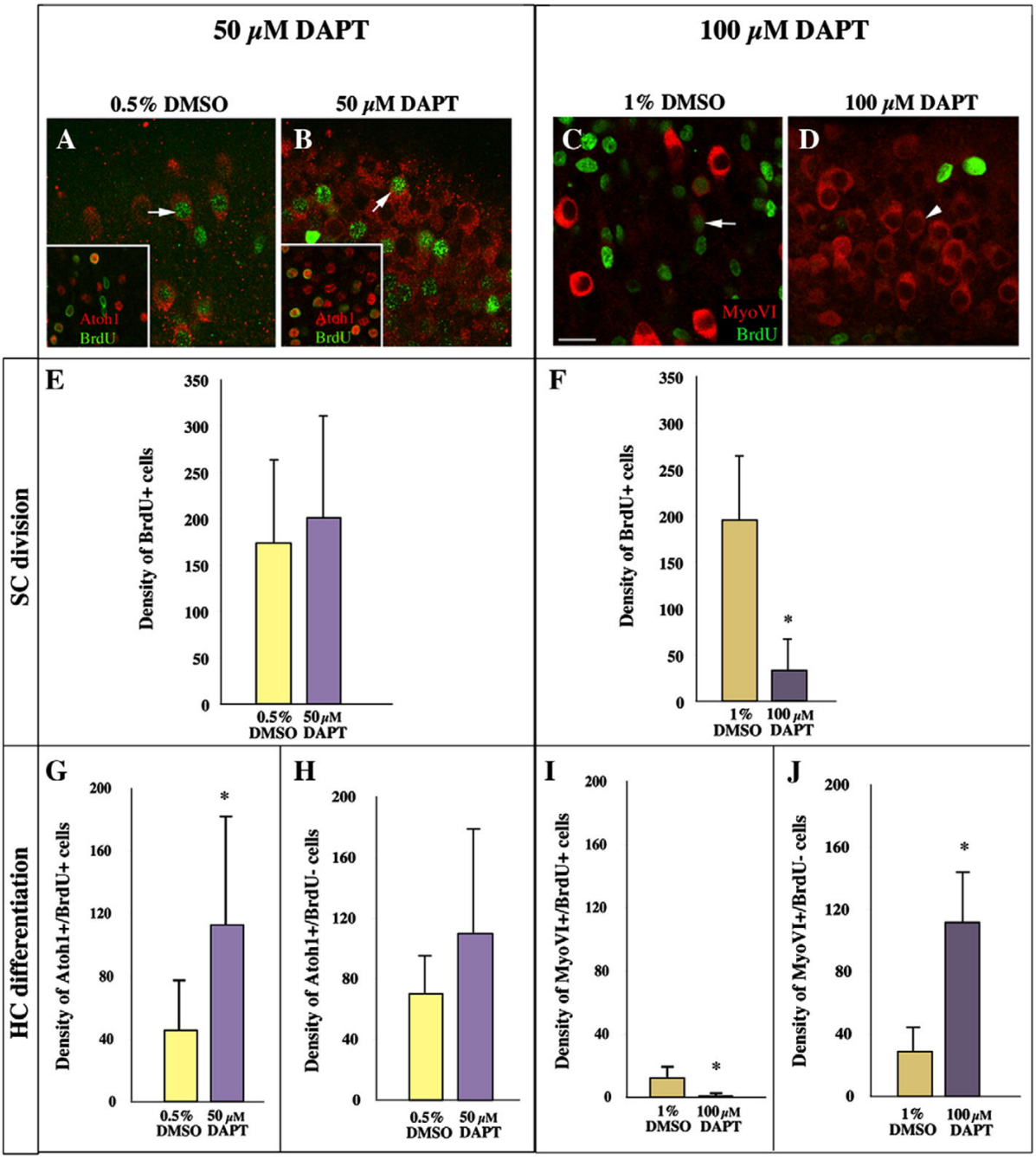

Figure 9. DAPT favors HC differentiation, and at the highest dose, can also limit SC division

A–D. These images show single confocal slices through the HC layer in the neural region of BPs treated with 0.5% DMSO (A), or 50 μM DAPT (B), 1% DMSO (C), 100 μM DAPT (D). In each case, 2 days of Streptomycin were followed by 6 days in DAPT/DMSO, with BrdU present throughout. BrdU immunolabeling is shown in green in all images, while MyosinVI immunolabeling is shown in red in A–D and Atoh1 immunolabeling is shown in red in the insets in A and B. Arrows in A–C point to post-mitotic regenerated HCs, which are double-labeled for BrdU and MyosinVI. The arrowhead in D points to a MyosinVI-positive (+) cell that is BrdU-negative (−). In the insets, cells that are double-labeled for Atoh1 and BrdU have orange nuclei, while those that are Atoh1+ and BrdU− have red nuclei. **E,F.** Quantitative

analysis of cell division. Graphs show the density of BrdU+ nuclei measured in BPs treated with 50 μM DAPT or 0.5% DMSO (E) and the density of BrdU+ nuclei measured in BPs treated with 100 μM DAPT or 1% DMSO (F). **G–J.** Quantitative analysis of HC differentiation. G,H. These graphs show the density of MyosinVI+/BrdU+ cells (new post-mitotic HCs)(G) or the density of MyosinVI+/BrdU− cells (new HCs formed by direct transdifferentiation)(H) measured in BPs treated with 50 μM DAPT or 0.5% DMSO. I,J. These graphs show the density of MyosinVI+/BrdU+ cells (new post-mitotic HCs)(I) or the density of MyosinVI+/BrdU− cells (new HCs formed by direct transdifferentiation)(J) measured in BPs treated with 100 μM DAPT or 1% DMSO. For all graphs, density = number of cells per 41,209 μm^2. All error bars are s.d.'s. Scale bar (in A) = 10 μm for A–D, 22 μm for insets in A and B.

Table 1

Primers for qRTPCR

Gene	5′ Sequence	3′ Sequence
Notch1	CACCGAAGGTTTCTCAGGTGT	GGCAGAGGCAGGTGAAGG
Notch2	GCTGCTCAGGCAATCAAGG	TGCCACGGCGAGTAGGTAG
Serrate1	TGCCAGACGGTGCTAAGTG	TCGAGGACCACACCAAACC
Serrate2	TGGAAGGTTGGATGGGAGA	CCTGGGTAGCGGACACACT
Delta1	GCAGGAGTGAAACGGAGACC	CGATGACGCTGATGGAGATG
Cath1	AACCACGCCTTCGACCAG	TGCAGCGTCTCGTACTTGGA
Hes5	TATGCCTGGTGCCTCAAAGA	GCTTGTGACCTCTGGAAATGG
Hes6	GATTCCAAAGTGGGCCTTGA	CTCGCAGGTGAGGAGAAGGT
MINT	GAGATCCATCCGCCCAGAC	ACAGCCCATCGAACACAGG
Lunatic fringe	GAAGAGCTGCGGGAGGAAG	GCTCCACCATGAGCACCAG
MyosinVI	TTCCTGCCGAAGAGGACAG	TGTGGAGGAGAGTGGCTTCA
β-Tectorin	GGCCCTGCACTCCAAATAAA	AGCTGATTGACCTCCCATCC